AD-A142 037 FRAZIL ICE DYNAMICS(U) COLD RGGIONS RESEARCH AND ENGINEERING LAB HANOVER NH S F DALY APR 84 CRREL-MONO-84-1 1/1

UNCLASSIFIED F/G 8/12 NL

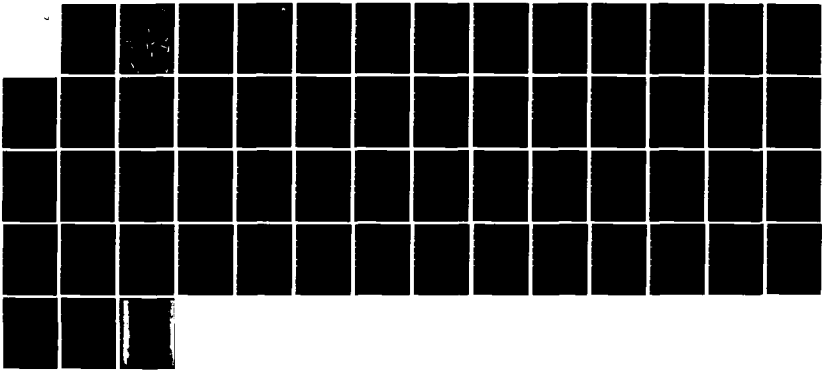

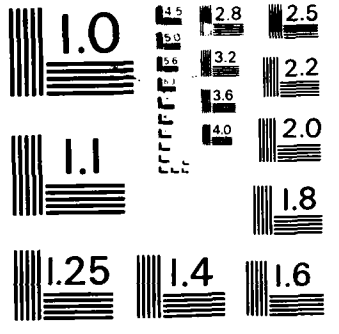

CRREL
MONOGRAPH 84-1

US Army Corps
of Engineers
Cold Regions Research &
Engineering Laboratory

Frazil ice dynamics

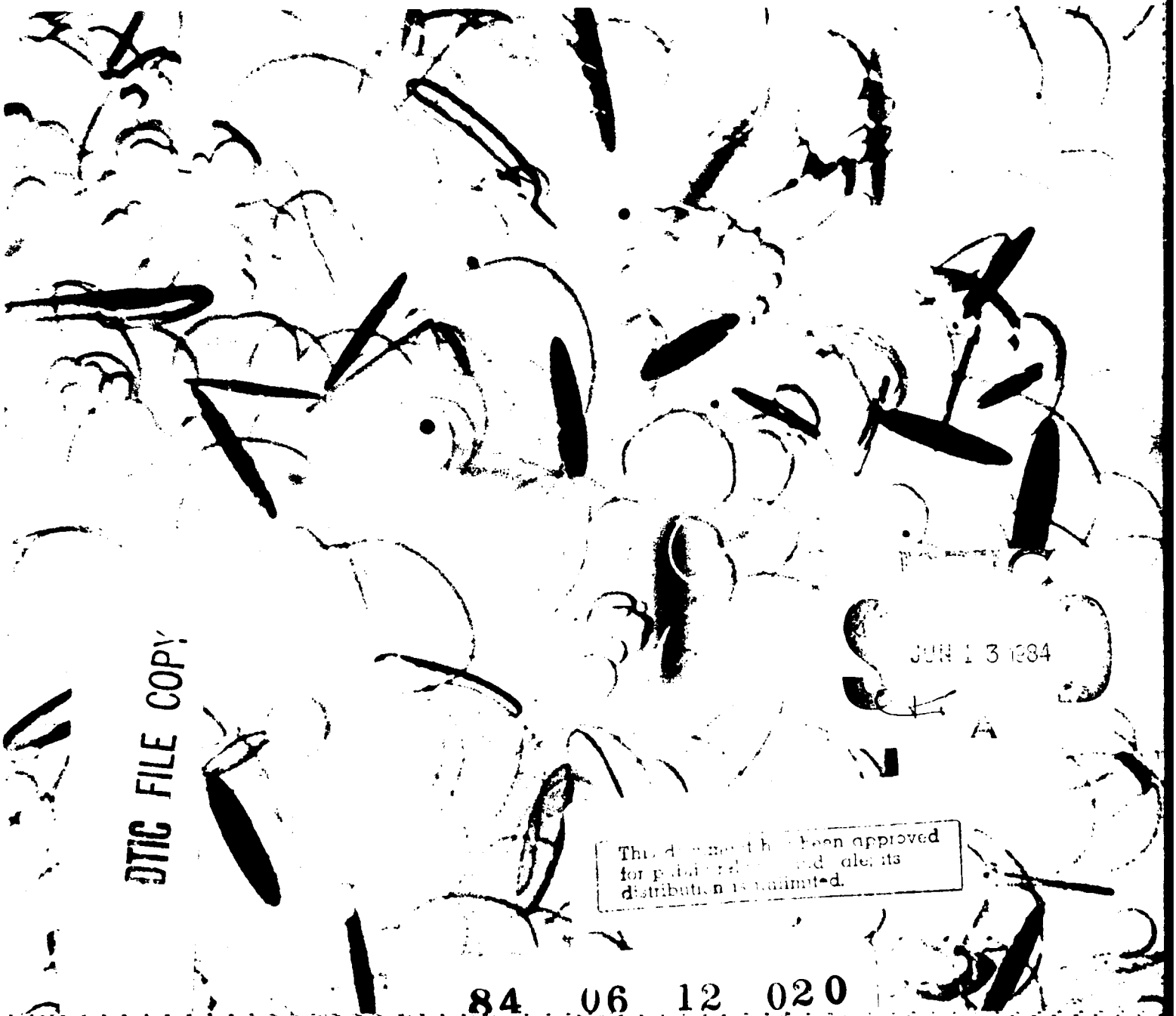

For conversion of SI metric units to U.S./British customary units of measurements consult ASTM Standard E380, Metric Practice Guide, *published by the American Society for Testing and Materials, 1916 Race St., Philadelphia, Pa. 19103.*

Cover: Magnified frazil ice crystals.

CRREL Monograph 84-1

April 1984

Frazil ice dynamics

Steven F. Daly

Unclassified

SECURITY CLASSIFICATION OF THIS PAGE *(When Data Entered)*

REPORT DOCUMENTATION PAGE

READ INSTRUCTIONS BEFORE COMPLETING FORM

1. REPORT NUMBER: MONOGRAPH 84-1	2. GOVT ACCESSION NO.
3. RECIPIENT'S CATALOG NUMBER	
4. TITLE *(and Subtitle)*: FRAZIL ICE DYNAMICS	5. TYPE OF REPORT & PERIOD COVERED
	6. PERFORMING ORG. REPORT NUMBER
7. AUTHOR(s): Steven F. Daly	8. CONTRACT OR GRANT NUMBER(s)
9. PERFORMING ORGANIZATION NAME AND ADDRESS: U.S. Army Cold Regions Research and Engineering Laboratory, Hanover, New Hampshire 03755	10. PROGRAM ELEMENT, PROJECT, TASK AREA & WORK UNIT NUMBERS: CWIS 31724
11. CONTROLLING OFFICE NAME AND ADDRESS: Office of the Chief of Engineers, Washington, D.C. 20314	12. REPORT DATE: April 1984
	13. NUMBER OF PAGES: 56
14. MONITORING AGENCY NAME & ADDRESS *(If different from Controlling Office)*	15. SECURITY CLASS. *(of this report)*: Unclassified
	15a. DECLASSIFICATION/DOWNGRADING SCHEDULE

16. DISTRIBUTION STATEMENT *(of this Report)*

Approved for public release; distribution unlimited.

17. DISTRIBUTION STATEMENT *(of the abstract entered in Block 20, if different from Report)*

18. SUPPLEMENTARY NOTES

19. KEY WORDS *(Continue on reverse side if necessary and identify by block number)*

Crystal growth
Crystallization
Frazil ice
Ice
Ice formation
Ice prevention
Mathematical analysis

20. ABSTRACT *(Continue on reverse side if necessary and identify by block number)*

To describe the dynamic evolution of frazil ice in turbulent natural water bodies, the basic equation for dynamic frazil crystal number continuity and the basic equation of heat balance for a differential volume are developed. Crystal growth and nucleation of new crystals are the major parameters in these equations. Expressions for the growth rate of frazil ice crystals are described. The growth rate along the major axis is controlled by heat transfer. The heat transfer coefficient is a function of crystal size, the fluid turbulence, and the fluid properties. The magnitude of inertial and buoyancy forces on the ice crystals are determined as is their influence on the heat transfer. Spontaneous nucleation of ice can be discounted; secondary nucleation is responsible for the vast majority of frazil ice crystals. The theoretical rate of secondary nucleation is partially modeled as a function of the supercooling, fluid turbulence and crystal size distribution. A simple analytical solution of the basic equations is developed for the growth of frazil ice in a well-mixed, steady-state crystallizer.

DD FORM 1 JAN 73 1473 EDITION OF 1 NOV 65 IS OBSOLETE

Unclassified

SECURITY CLASSIFICATION OF THIS PAGE *(When Data Entered)*

PREFACE

This monograph provides a technical analysis of the state of the art in some facets of the physics of frazil ice. One of the intentions of the *CRREL Monograph* series is to provide such updates and introductions in various aspects of cold regions science and technology.

This monograph was prepared by Steven F. Daly, Research Hydraulic Engineer of the Ice Engineering Research Branch, Experimental Engineering Division, U.S. Army Cold Regions Research and Engineering Laboratory, under the guidance of Dr. Keith Stolzenbach, Associate Professor of Civil Engineering, R.M. Parsons Laboratory for Water Resources and Hydrodynamics, Massachusetts Institute of Technology. It was prepared by the author at the Massachusetts Institute of Technology and was submitted to the Department of Civil Engineering in September 1982 in partial fulfillment of the requirements for the Degree of Master of Science in Civil Engineering. Funding was provided by Civil Works Research Area, *Flood Control and Navigation;* Research Program, *Ice Engineering;* Work Unit CWIS 31724, *Frazil Ice Control for Field Use.*

The author wishes to acknowledge the key role of Dr. Stolzenbach in the preparation of this report. In addition, the many fruitful discussions with the faculty and students of MIT and researchers of CRREL are appreciated.

NOMENCLATURE

a	Constant
a_1, a_2, a_3	Constants
a', a''	Linearized intrinsic kinetic growth rate constants
$\vec{A}_f$	Acceleration of fluid
$\vec{A}_R$	Relative acceleration of crystal and fluid
A_s	Surface area of disk
A_T	Total surface area of crystals in R
$a(r)$	Area of crystal of size r
b	Constant
B	Birth function
C	Heat capacity of fluid
C_D	Drag coefficient
C_T	Fluid impurity concentration
C_i	Heat capacity of ice
D	Death function
E_{rb}	Collision energy created by collisions of crystals and boundaries
$\vec{E}$	Pure straining motion of fluid
E_w	Fluid strain rate along crystal rotation axis of symmetry
$E(r_1, r_2)$	Collision energy created by collisions of crystals of size r_1 and r_2
$\dot{E}_t$	Rate of energy transfer by collision
F_1	Number of particles generated per unit of collision energy
F_2	Fraction of particles surviving to become crystals
F_D	Drag force
g	Gravity
g'	Reduced gravity
G	Crystal growth rate
G_k	Kinetic growth rate
h	Heat transfer coefficient
h_e	Heat transfer coefficient from disk edge
h_f	Heat transfer coefficient from disk face
k	Thermal conductivity of water
K_a	Geometric shape factor
K_v	Volumetric shape factor
L	Mean latent heat of fusion of ice
L_{te}	Latent heat of fusion of ice as a function of the equilibrium temperature
m^*	Nondimensional crystal size
$m(r)$	Mass of crystal of size r
M_T	Total mass of crystals in R
n	Size distribution function

CONTENTS

ILLUSTRATIONS

U_t	Terminal rise velocity
$\bar{v}$	Velocity after collision of combined mass of crystals of size r_1 and r_2
$v(r_1, r_2)$	Relative velocity of crystals of size r_1 and r_2
$\vec{V}_e(R, t)$	External phase space convective velocity of crystal
$\vec{V}_f$	Fluid velocity
$\vec{V}_i(R, t)$	Internal phase space convective velocity
$\vec{V}(R, t)$	Phase space velocity
$V(t)$	Volume of well-mixed crystallizer at time t
X	Particle added mass
$\vec{X}_{ij}$	Position vector
α	Thermal diffusivity
α_T	Turbulent intensity
β	Heat transfer disk factor
γ	Ice/water interfacial tension
ϵ	Turbulent dissipation rate
η	Dissipation length scale
θ	Bulk supercooling
θ_i	Supercooling at the crystal interface
υ	Fluid kinematic viscosity
ρ_f	Density of water
$\hat{\rho}_f$	Mass concentration of water in mixture
$\hat{\rho}_i$	Mass concentration of ice in mixture
ρ_i	Density of ice
Φ	Dissipation function
$\Psi(r_1, r_2)$	Collision efficiency of crystals of size r_1 and r_2
$\vec{\Omega}$	Solid body of rotation of fluid
τ	Crystallizer flow through time
ℓ	Length scale of eddy
ℓ_m	Length scale of maximum eddy size

n_K	Population density of the K^{th} input and output stream into crystallizer
n^0	Population density of newly nucleated crystals
N	Total number of crystals per unit volume
$\dot{N}$	Nucleation rate per unit volume
$\dot{N}_I$	Rate of introduction of new crystals
$N(r)$	Number
$\dot{N}_T$	Total secondary nucleation
Nu	Nusselt number
Nu_T	Turbulent Nusselt number
Nu_0	Nusselt number for a particle in a stationary fluid
Pe	Péclet number
Pr	Prandtl number
q	Rate of heat transfer per unit surface area
q_{rb}	Frequency of collision between crystals and boundary
$q(r_1, r_2)$	Frequency of collisions between crystals of size r_1 and r_2
Q^*	Net heat transfer
Q_K	Discharge rate of the K^{th} input and output stream into crystallizer
r	Major linear dimension of frazil crystals
$\bar{r}$	Mean crystal size
r^*	Nondimensional crystal size
r_e	Edge dimension of disk
r_f	Face dimension of disk
R	Region of phase space
R_c	Collision radius
Re	Reynolds number
R_h	Hydraulic radius
S	Fluid shear rate
S_N	$(F_1)(F_2)$
t	Time
T^*	Characteristic time
T_e	Temperature at interface due to surface curvature
T_f	Temperature of fluid
T_i	Temperature at interface due to intrinsic kinetics
T_{ice}	Temperature of suspended ice crystal
T_m	Ice-water equilibrium temperature
$T(r^*)$	Form of crystal size distribution assumed constant with time
T_s	Temperature at surface of a suspended particle
u	Eddy velocity
u'	Turbulent fluctuation of velocity
u^*	Characteristic eddy velocity
$\vec{U}_p$	Particle velocity
U_{rb}	Relative velocity of crystal and boundary
U_R	Relative velocity of crystal and fluid

FRAZIL ICE DYNAMICS

Steven F. Daly

INTRODUCTION

Frazil ice, fine spicule, plate or discoid crystals in supercooled turbulent water, is commonplace on many northern rivers and lakes during the winter, but the processes that create it are not well understood. Frazil is formed when heat is withdrawn from a body of turbulent water that is at the freezing point. The temperature of the water follows a qualitatively well-known sequence: it falls below the freezing temperature to a minimum and then returns to the freezing point. This temperature sequence represents a dynamic balance between the latent heat released by the growing frazil ice crystals and the heat lost to the environment from the water.

Frazil ice can block water supply intakes, hydroelectric plant intakes, irrigation and water supply canals, and it can form ice jams that can block an entire river cross section and cause extensive flooding. Although the adverse effects of frazil cost the world uncounted millions of dollars each year, currently no quantitative estimates about any aspect of this sequence of frazil formation can be made. The deficiencies in the current state of knowledge are "severely hindering development of rational design methods for avoidance or alleviation of frazil ice problems" (ASCE Task Committee 1974).

There exists then an obvious need for a comprehensive, physically based quantitative model of the basic processes that control and direct the growth of frazil in natural water bodies. The slow development of such a model has been frustrating to the engineers who must cope with the unique problems of frazil. Despite such provocative statements as "the phenomenon of frazil... is similar to the more general one of crystallization in a supersaturated medium" (Michel 1963), very seldom has an attempt been made to study frazil in the wider context of crystal growth from a solution. The problems of large-scale industrial crystallization, however, can provide insight into the frazil problem.

The goal of this report is to take the first steps toward development of a comprehensive, quantitative model of the process of frazil formation by relating knowledge of industrial crystallization to the conditions present in natural water bodies. Toward this end, this paper develops the mathematics needed to describe the dynamic interaction of the frazil ice crystal distribution and the heat balance of the turbulent water.

The *Literature Review* section covers frazil ice in natural water bodies, and industrial crystallization.

The *Basic Equations* section describes the dynamic crystal number continuity equation in particle phase space and the basic equation determining the heat balance of the water. Also defined are the moment equations defining the total crystal number, area and volume.

In the *Ice Crystal Growth Rates* section, the growth rate along the *a*-axis (the major growth axis) is found to be controlled by heat transfer. The heat transfer coefficient for disk-shaped particles is determined as a function of crystal size and level of fluid turbulence. The magnitudes of the inertial forces and buoyancy forces on the ice crystals are determined and their influence on the heat transfer assessed. It is concluded that inertial forces can be neglected but that gravity forces may become significant for large crystals in weak turbulence.

The *Nucleation* section discusses both initial nucleation and secondary nucleation of frazil. It is concluded that spontaneous nucleation of ice can be discounted, and that seed crystals are needed to begin frazil growth. The theoretical rates of secondary nucleation are partially modeled, and they are found to depend on the level of supercooling, the turbulence level and the crystal size distribution.

The *Frazil Ice Dynamics* section presents a simple but practical analytical solution of the basic equations for a steady-state crystallizer, and the results are presented for the growth of frazil in such a crystallizer. An overview of the basic equations is presented emphasizing the information feedback inherent in the equations. The next steps in future research are outlined.

LITERATURE REVIEW

Introduction

Either directly or indirectly, frazil ice has drawn the attention of numerous engineers and scientists, and the literature comes from many fields. The first part of this section is a brief chronological review of the literature produced by civil and mechanical engineers, who are concerned with frazil ice in northern rivers and lakes, the meteorological and hydraulic conditions under which it formed, and its tremendous negative impact on man's activity. The second part of this section reviews knowledge gained about frazil from other approaches, primarily from interest in the desalination of sea water by freezing. In this context, frazil is viewed as an industrial product that is made in bulk crystallizers. *This will not be a* chronological review, but rather an introduction to the extensive literature on industrial crystallization.

Frazil ice in natural water bodies

Interesting phenomena such as ice forming on fishing lines and baskets under water, lost anchors being lifted by masses of ice, and ice displacing buoys by moving their moorings brought early attention to frazil ice. But frazil was not studied seriously until people began to use rivers and lakes uninterrupted throughout the winter. Hydropower, winter navigation and demands for fresh water by factories and cities provided economic incentives for the study of frazil ice.

Research on frazil ice in natural water bodies was produced in response to several major concerns. The first was predicting where frazil ice would form. The ability to do this is vitally important to those who must keep open the water intakes of hydroelectric plants, water supplies, etc. A second was predicting the total volume of frazil ice that a given reach of river could produce because large volumes of frazil often cause dam-like ice jams that can cause catastrophic flooding. A third major concern was coping with the problems caused by frazil, primarily finding ways of keeping intakes operating, keeping canals and navigation channels open, and eliminating ice jams.

The meteorological and hydraulic conditions under which frazil can form were determined through observation and hard experience. Murphy (1909) provided a good description of these conditions. Two of his points, that frazil forms in areas where an ice cover does not exist and that it is closely associated with turbulent waters, are universally recognized.

In *Ice Engineering*, Barnes (1928) summarized the knowledge of ice formation up to that time, and promulgated certain ideas about the formation of frazil. Many of Barnes' ideas were not correct. Unfortunately, these misconceptions displayed a "remarkable persistence" (Carstens 1966) and many years passed before they were totally rectified. Barnes did, however, firmly establish that there was always supercooling during the formation of frazil.

After the publication of *Ice Engineering* in 1958, European investigators took the lead in frazil research. Altberg in Russia and Devik in Norway. Ice research in Russia had been stimulated by a major frazil ice completely blocked the water supply of the city of St. Petersburg in 1914. Both Devik and Altberg emphasized quantitative accounting of heat transfer and advanced more correct ideas on the mechanisms of ice nucleation and the role of long-wave heat transfer. Both believed that water particles suspended in the water provide nuclei for the ice. Both emphasized the need for supercooled water and demonstrated that water bodies producing frazil ice were indeed supercooled. Devik (Carstens 1966) is credited with introducing the terms "active" and "passive" to distinguish frazil ice in supercooled water (active) from frazil ice in water at the freezing point (passive). Active frazil has a greater tendency to stick to submerged objects than passive frazil. Altberg (1936) noted that ice crystals introduced into supercooled turbulent water produced a great number of additional crystals, and suggested that portions of the crystals may break off and serve as the start for a new growth of crystals. This idea, which has been expanded into the theory of secondary nucleation, will be discussed in a following section.

At the 1959 Montreal Congress of the International Association of Hydraulic Research (IAHR), the Committee on Ice Problems was created. Therefore, the 1950's can serve as a convenient, if arbitrary, division between the early and recent literature. Seminars on ice problems were held at the IAHR Congresses through the 1960's. In 1970 the first International Symposium on Ice Problems was held in Iceland, and since then they have been held regularly (1970, 1972, 1975, 1978, 1981). Many excellent papers on frazil are contained in the proceedings of these symposia.

Detailed observations of frazil formation in small streams were published by Schaefer (1950) and Gilfillian et al. (1972). Wigle (1970) and Arden and Wigle (1972) published detailed observations of frazil formation in the Niagara River. Schaefer observed that frazil crystals appeared to form initially on the water's surface and were then submerged by turbulence. He found that the frazil crystals retained their disk shape up to a diameter of approximately 2-3 mm but beyond this dimension dendrites grew out from the flat disks. He noted that these dendrites were quite fragile and easily detached. He described sponge-like deposits of frazil that gather on the upstream side of rocks and other underwater objects, but he drew a distinction between this and "true" anchor ice - true anchor ice being sheet-like crystals of ice that grew out from submerged objects to which they were securely fastened. Schaefer felt that true anchor ice was quite rare in nature and that almost all reported anchor ice was actually deposited frazil.

Gilfillian et al. (1972) closely observed the freezeup of a small subarctic Alaskan stream. The border along the edge of the stream grew inwards to cover it 5 days after freezeup began. They measured an increase in the electrical conductivity of the stream water during the periods of frazil production and they attributed this to the rejection of impurities by the ice during growth of the ice crystals. They found substantial agreement between the mass of frazil determined by estimating the heat loss from the stream and the mass of frazil determined from the increase in electrical conductivity. The initial ice crystals at the start of a period of supercooling were discoids, six-pointed stars or hexagonal. Frazil crystals larger than 1 mm in diameter had scalloped edges or were irregularly shaped.

Arden and Wigle (1972) observed frazil formation on the upper Niagara River, a large, fast flowing river that remains open all winter. They determined a "typical" sequence of ice formation that took place each night when meteorological conditions allowed the heat content of the river to dissipate. During such a typical sequence, the river cooled from the surface down. They saw crystals on the surface even when the temperature of the main body of the river was +0.03 C. As the main body of the river cooled, the crystals on the surface became larger and were submerged to greater depths by the turbulence. Some of the crystals on the surface were disks, but most were irregular. There was a "transition" period, lasting about 1 hour, during which the top 2-3 m of water was supercooled while the bottom 5-7 m retained a temperature slightly above freezing. Frazil appeared in the supercooled layer but not in the lower layer; however, when the entire river became supercooled, frazil existed throughout the depth of the river. During this period disk-shaped crystals were the dominant form.

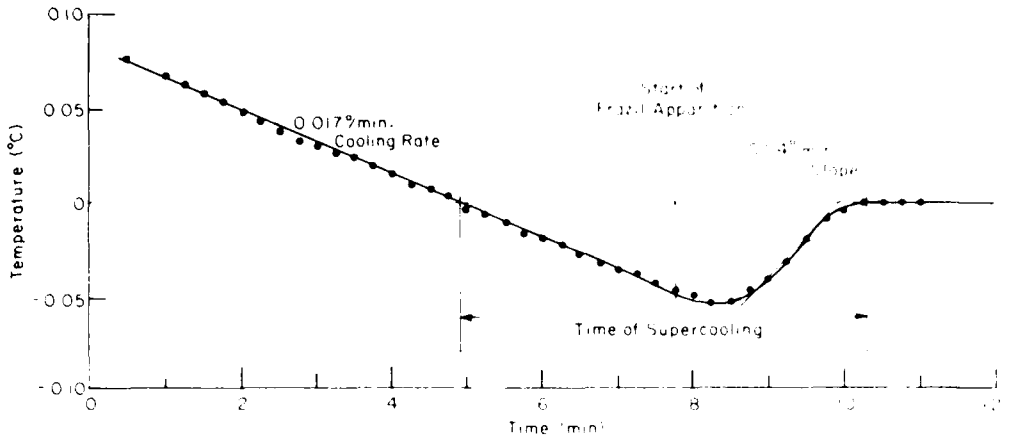

Figure 1. Typical supercooling sequence (after Michel 1967).

The frazil in the supercooled water immediately stuck tenaciously to any submerged object. However, frazil did not build up on the river bottom until the supercooled water had existed for a few hours. During a typical night this anchor ice buildup reduced the flow of the river by as much as 25%.

Beginning in the 1960's a series of experiments were conducted in flumes by Michel (1963) and Carstens (1966) that provided very consistent qualitative descriptions of frazil formation. Michel (1963) determined a typical sequence of water temperatures and frazil formation (Fig. 1). At the start of such a sequence the water in the flume cooled at a constant rate. A time history of the water temperature formed a straight line with constant negative slope during this initial period. When the water temperature reached 0°C, it passed through this temperature and continued cooling at the same rate until it reached a few hundredths of a degree below the freezing point, after which the rate of temperature drop began to decrease rapidly until it became zero. At this time tiny ice particles formed that were too small to be seen by the naked eye, but could be detected if viewed with a strong light.

After the water reached its minimum temperature, it returned to 0°C. Initially, the water temperature would rise quickly and then more and more slowly, approaching 0°C asymptotically. The water temperature measured by Michel during the course of an experiment reflected a balance between the heat loss at the water's surface and the latent heat released by the growing frazil crystals. When the rate of temperature change became zero, the latent heat released by the growing crystals exactly balanced the heat loss at the water surface.

Carstens (1966) conducted a series of experiments in a test flume where he investigated the extent to which water could be supercooled. He varied the rate of heat loss through the water surface and he varied the turbulence of the flow. Carsten's experiments produced temperature-time history curves very similar to those of Michel. However, the temperature of the water did not always return to the freezing point; it would often reach a constant value of supercooling, which he termed the residual supercooling. When the rate of heat loss from the water surface was increased, the maximum supercooling of the water increased, the residual supercooling increased and the rise in temperature from the maximum supercooling to the residual supercooling required less time. Carstens also felt that the number of ice crystals increased. He saw large qualitative differences in the temperature-time history curves when the turbulence of the flow was varied. "Strong" turbulence produced relatively small maximum supercooling levels, and the temperature would return relatively quickly to the freezing point with little or no residual supercooling, while "weak" turbulence produced relatively large maximum supercooling levels that would persist for relatively long periods.

Carstens concluded that the level of supercooling reached in a particular experiment reflected the balance of the heat loss at the surface and the heat transferred from the growing frazil crystals,

which was controlled by turbulence of the flow. He suggested that the heat transfer from the particles to the water could be related by an expression such as $Nu = C'Re^m$ where Nu is the Nusselt number (nondimensional heat transfer), C and m are physical constants in his nomenclature, and Re is the Reynolds number based on the characteristic velocity of the flow and the characteristic linear dimension of the frazil crystal.

The final experiments inspired by observations of frazil in natural water bodies to be described in this section are those of Muller (1978). Muller conducted his experiments in a refrigerated turbulence jar in which turbulence was generated by an oscillating grid. He investigated the rate of heat transfer from the frazil crystals to the supercooled water and the rate at which the number of frazil crystals increased. He observed no frazil at supercooling levels up to 1 C unless the water was seeded with ice crystals.

The number of ice crystals increased during the course of an experiment. Muller concluded that some type of multiplication process was at work, but he could gain no insight into the mechanisms of this process. However, the multiplication process "intensified" with an increase in supercooling or an increase in turbulence. He found that the apparent heat transfer from the frazil crystals could be normalized with the supercooling level and the size of the crystals and that it was a constant for all the experiments with an average representative value of the Nusselt number of 10.

Many studies have attempted to predict the total volume of frazil that can be produced in natural water bodies by estimating the heat budget of the water body. Freysteinsson (1970) and Carstens (1970) presented generalized approaches. Basically, these involved determining the heat budget by accounting for the total heat transfer at the water surface by evaporation, convection and radiation, and the heat transfer from other sources, such as through the bed and viscous generation of heat. These researchers found that the most heat was transferred through the water surface, and that the other sources could generally be ignored. They assumed that once the water temperature reached the freezing point, any additional heat loss resulted in the production of frazil. A general relationship, $M = QA/L$, was used to calculate M, the mass of frazil, where L is the latent heat of fusion, Q the total heat loss per unit area, and A the surface area of the water body.

Estimates of the amount of frazil generated in the Niagara River were made by Ferguson and Cork (1972) and List and Barrie (1972). Shen (1980) and Shen and Ruggles (1982) made very detailed estimates of the volume of frazil generated in the open sections of the St. Lawrence River. In all these studies heat losses at the water surface dominated the heat budget of the water. Shen found that the bed heat flux could be an important component, especially for colder winters when the open water area was small.

In this section a brief review of the civil engineering literature relevant to frazil has been presented. The important question of the initial nucleation of frazil, which has been long debated, will be discussed later in a separate section. The specific problem of ice control at water intakes was not mentioned, although there is literature on the subject (Murphy 1909, Granbois 1953, Logan 1974, Tantillo 1981). In addition, several very good general reviews of frazil have been published (Williams 1959, Michel 1971, Osterkamp 1978, Ashton 1978, Martin 1981).

Frazil ice in industrial crystallizers

Other than in natural water bodies, frazil has been extensively studied only in the industrial crystallization process of desalination by freezing. Industrial crystallization is the production of crystals from supersaturated or supercooled solutions in agitated vessels of varying complexity that are called crystallizers. Generally, the average crystal size and crystal size distribution are very important in determining the economic returns of a crystallizer product. Therefore, investigators have expended much time and effort in developing both theoretical and empirical means of predicting the crystal size distribution that will result from a given crystallizer. A good introduction to this is *Theory of Particulate Processes* (Randolph and Larson 1971). The rigorous determination of the crystal distribution, together with the associated heat balance and the appropriate boundary conditions, provides a unified predictive and descriptive theory for desalination by freezing.

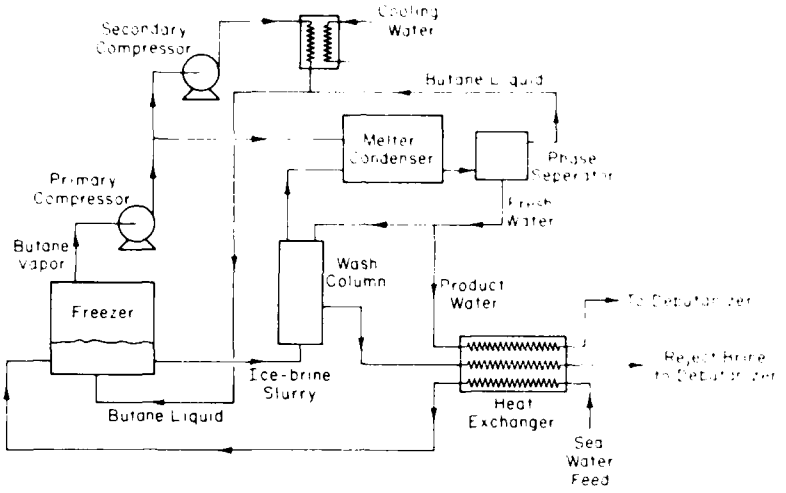

a. Butane freezing process, simplified flow diagram.

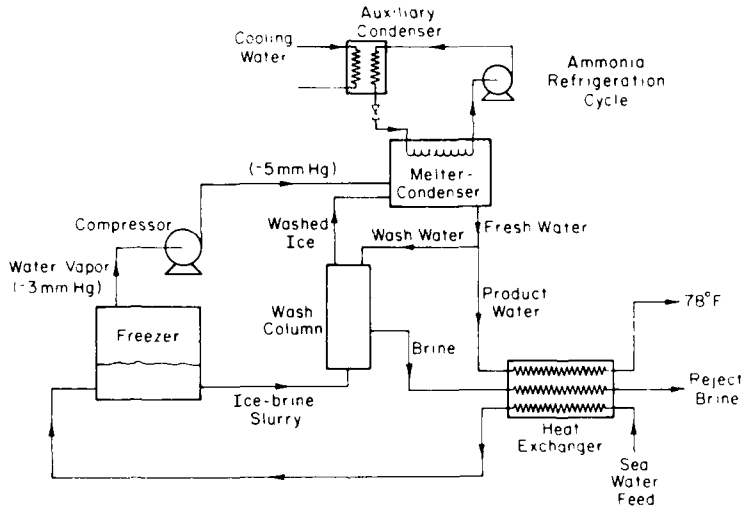

b. Vacuum flash freezing process, simplified flow diagram.

Figure 2. Desalination by freezing.

Desalination by freezing

Desalination by freezing has been extensively studied (Margolis 1969, Kane 1971, Evans 1973, Simpson et al. 1973, Woltz 1975, and Smith and Sarofim 1979). Desalination by freezing is predicated on the low solubility of salt in ice. The ice is formed in an agitated crystallizer from which heat is removed; the supercooling levels achieved in the crystallizers are small, typically less than 1°C. The dominant shape of ice formed is a disk. The resulting ice-brine slurry is pumped to a washer where the brine is drawn off. The ice is then melted by the condensing refrigerant.

There are several methods for removing heat from the crystallizer. The secondary refrigerant freezing process removes heat by vaporizing an immiscible refrigerant, such as butane. The vacuum freezing-vapor compression process vaporizes a portion of the brine at low pressure. Both processes are shown in Figure 2.

In desalination by freezing, the quality of the crystallizer product and the production rate largely determine the economic returns of the process. The product quality is determined by the average crystal size and the crystal size distribution, and it is important in determining the pressure drop

across the ice bed formed in the washer because the pressure drop is inversely proportional to the square of the crystal diameter. Also, the melting rate of the crystals increases as the crystal size increases. Therefore, the quality is improved when the average size is increased and when the number of small particles is decreased. The production rate is equal to the crystallizer volume times the slurry density divided by the average residence time of the ice in the crystallizer. Thus the production rate can be improved if the slurry density is increased, if the average crystal size is increased or if the residence time is decreased.

Generally, the type of crystallizer proposed for this process would operate at steady state and is called a Mixed Suspension, Mixed Product Removal (MSMPR) crystallizer. Operation at steady state requires that the number of crystals and the crystal size distribution do not change with time. New crystals must be nucleated in the crystallizer as the crystallizer is operated with clear (unseeded) feed streams. At steady state, one crystal must be nucleated for each crystal in the crystallizer in an average of one residence time. Therefore, the residence time is equal to the number of crystals (N) divided by the nucleation rate present in the crystallizer ($\dot{N}$). The average crystal size can be determined by multiplying a representative growth rate (G) of the crystals by the average residence time. The average crystal size ($\bar{r}$) is then

$$\bar{r} = GN/\dot{N}.$$

The average crystal size is a function of the nucleation and growth rates. The nucleation rate and the growth rate are therefore very important in determining the economics of desalination by freezing.

Nucleation rate

The type of nucleation in ice crystallizers is secondary nucleation, and secondary nucleation takes place, irrespective of its mechanism, only because of the presence of crystals of the material being crystallized (Botsaris 1976). For secondary nucleation to occur, the existing stable crystals must in some way generate new crystals. Inquiry into this process can be conveniently divided into two questions: what is the source of the potential nuclei of the new crystals and how are these nuclei removed from the source and displaced into bulk solution to initiate new crystals?

A number of sources of the ice nuclei have been suggested, including dendrites, microscopic surface irregularities and large-scale breakage of the parent crystal. Dendrites and surface protuberances are often reported on frazil crystals and, if detached from the parent crystal, could easily initiate new crystals. However, there is ample evidence that secondary nucleation can happen without visible dendritic growth (Evans 1973, Woltz 1975). Clontz and McCabe (1971) were able to generate crystal nuclei by causing crystals to collide with rods of various materials. The contacts produced no visible defects in the parent crystals, but they assumed that during the collisions microscopic surface irregularities were sheared off. These microscopic particles are considered the most likely source of potential ice crystal nuclei (Evans et al. 1974a, b). Large-scale breakage of ice crystals is rarely observed.

The production of the crystal nuclei from the sources described above has been attributed to fluid shear and collisions of all types. Clontz and McCabe (1971) found no evidence that fluid shear could produce new crystals. Secondary nucleation induced by collisions among the parent crystals has been investigated by Lal et al. (1969), Garabedian and Strickland-Constable (1972), Ottens et al. (1972), Denk and Botsaris (1972) and Desai et al. (1974). Secondary nucleation of ice crystals by collision with other surfaces has been investigated by Garabedian and Strickland-Constable (1974), Evans et al. (1974a, b), and Woltz (1975). The number of crystals produced per collision was found to increase with the collision energy and the supercooling of the fluid.

Garabedian and Strickland-Constable (1974) proposed the survival theory to explain these results. According to the survival theory, the number of nuclei produced per collision is proportional to the collision energy and independent of the supercooling level. The nuclei produced are distributed over a range of sizes, and only those larger than a critical radius, determined by the supercooling

of the solution, survive and grow. Recent observations (Garside and Larson 1978) have produced doubts about some of the details of the survival theory; however, the models of secondary nucleation based on its premises are very general and can incorporate these results.

The rate of production of new crystals by secondary nucleation can be limited by either the production rate of the potential nuclei on the crystal surface or the rate of their removal from the crystal surface. Being limited by the removal rate implies that the time between collisions is long enough to allow the crystal surface to heal from previous collisions, so the nucleation rate is therefore independent of the system history. The secondary nucleation of ice is limited by the removal rate. Evans et al. (1974b) proposed that the overall nucleation rate ($\dot{N}_T$) for ice with more than one mechanism of removal is the linear sum of the actual nucleation rate attributable to each mechanism of removal. Thus

$$\dot{N}_T = \dot{N}_1 + \dot{N}_2 + \dot{N}_3 + \ldots \dot{N}_i$$

where $\dot{N}_i$ is the nucleation rate attributable to the ith mechanism.

For example, in a crystallizer, the overall nucleation rate is the linear sum of the nucleation rate caused by collisions of the ice crystals with the agitator (propellor or turbine), the crystallizer walls and other crystals. Evans et al. (1974b) demonstrated that coating the agitator and crystallizer walls with a material that is softer than ice could reduce the nucleation rate. The coating reduced the contact energy, thereby reducing the number of nuclei produced per collision.

Crystal growth rates

The growth of crystals in agitated turbulent solutions has long been a topic of research by chemical engineers. An extensive review is provided by Wadia (1974). The growth mechanisms for ice crystals suspended in supercooled water are the incorporation of water molecules into the ice surface (the crystalline kinetics) and the transport of the latent heat of fusion to the bulk fluid. Thus, the overall growth rate of an ice crystal, in fresh or salt water, is the result of the interaction of the crystalline kinetics and the transport processes of the surrounding turbulent fluid. It has been found that the growth rates of the major axis of disk crystals are largely controlled by transport processes. The transport processes can be described if the geometry of the crystal is known and if the ambient velocity distribution of the fluid in the vicinity of the crystal can be adequately described.

Unfortunately, the fluid in a highly agitated crystallizer exhibits a turbulent flow field with many seemingly random aspects. However, successful transport correlations predicated on Kolmogorov's theory of isotropic turbulence (Hinze 1959) have been developed. In a turbulent crystallizer, the impeller adds a known amount of energy and creates isotropic turbulence around the suspended crystals. The ambient velocity distributions are then determined by the energy put in by the impeller, the viscosity of the fluid and the crystal diameter. The transfer processes are calculated by determining the heat transfer given the ambient velocity distribution. The specific case of heat transfer from suspended frazil crystals will be described in more detail in the *Ice Crystal Growth Rates* section.

Summary

In summary, desalination by freezing is a process of industrial crystallization in which frazil ice is purposefully created to make fresh water from salt water. To provide the maximum economic return, the crystal size distribution has to be optimized as described. The two major influences on the crystal size distribution are the growth rate and the rate of secondary nucleation of the ice crystals, and as a result, the basic mechanisms that control these rates have been extensively researched. This research has not yet been applied to frazil production in natural water bodies

BASIC EQUATIONS

Introduction

In this section a descriptive and predictive crystal distribution theory, following Randolph and Larson (1971), will be developed. Rigorous determination of the population balance of crystals will result in a crystal number continuity equation, the solution of which is a distribution function that contains information about the form and the magnitude of the crystal distribution. The function describes the population density of crystals of each specific linear dimension throughout the volume. The physical parameters that affect the crystal size distribution appear in the crystal number continuity equation. An additional equation that describes the heat balance within the volume is required to determine the crystal size distribution. The two equations are linked by the growth and secondary nucleation rates of the ice crystals, which are dependent on both the heat balance and the crystal size distribution. In theory the equations can be solved if the various required boundary and initial conditions are known. These equations will serve as the framework for this investigation of frazil ice in natural water bodies. In addition, the crystal moment equations will be developed. These equations are very convenient for determining the total mass and surface area of the crystals as a function of size.

Crystal number continuity equation

The crystal distribution will be described in a space termed the crystal phase space or more generally the particle phase space. Particle phase space is defined by the least number of independent coordinates that provides a complete and useful description of the properties of the crystal distribution. It is convenient, if somewhat arbitrary, to divide particle phase space into two subregions defined by external coordinates and internal coordinates. The external coordinates describe the spatial distribution of the crystals. Internal coordinates refer to properties attached to each individual crystal, which quantitatively measure its state, and are independent of its position.

To begin, a crystal distribution function $n(R, t)$ will be considered. This function is defined over a region R of the particle phase space consisting of the three spatial dimensions (the external coordinates) plus any number of internal property coordinates. In all further cases the internal coordinates will be restricted to one, which will correspond to a major linear dimension, r, of the ice crystals. The function $n(R, t)$ is defined as the population density of crystals in the region R. At a time t the number of crystals in an incremental region of the particle phase space dR is given by

$$dN = n dR \tag{1}$$

and the total number of crystals in a region R at time t is

$$N(R) = \int_R n dR. \tag{2}$$

Individual crystals can continuously change their position in the particle phase space. If these changes are regular, that is, if they are the result of gradual and continuous movement, the convective crystal velocity along a respective particle coordinate can be defined. Let $\vec{V}_e$ be the external convective velocity and $\vec{V}_i$ be the internal convective velocity. $\vec{V}_e$ is the velocity of the crystal through space and will result from the interactions of all the forces acting on the crystal. $\vec{V}_i$, as restrictively defined here, simply represents the rate of change of the size of a crystal. The velocity of the overall vector crystal phase space is defined as

$$\vec{V}(R, t) = \vec{V}_e(R, t) + \vec{V}_i(R, t) . \tag{3}$$

It may also be necessary to deal with the sudden appearance (birth) or disappearance (death) of crystals at a point in the particle phase space. For example, the breakage of a crystal would cause the sudden disappearance of a crystal at the internal coordinate corresponding to its size and the sudden appearance of its fragments at the coordinates corresponding to their sizes. The net appearance in an incremental region dR at a time would be

$$(B-D)dR \tag{4}$$

where $B(R, t)$ and $D(R, t)$ represent birth and death functions at a point in the phase space.

The population balance of crystals in some fixed region R, which moves convectively with the particle phase space velocity V, can be defined as

$$\frac{d}{dt}\int_R n\,dR = \int_R (B-D)dR\,. \tag{5}$$

Expanding the first term using Leibnitz's rule, and noting that the region R was arbitrary, we can state the population balance in general terms as

$$\frac{\partial n}{\partial t} + \nabla(\vec{V}_e n) + \nabla(\vec{V}_i n) - B + D = 0\,. \tag{6}$$

This is the number continuity equation in particle phase space. This equation is quite general, as each term is defined over the three spatial coordinates, the internal coordinate r and time. As only a single internal coordinate r is considered, the divergence of the internal convective velocity can be represented as

$$\nabla(\vec{V}_i n) = \frac{\partial}{\partial r}(Gn) \tag{7}$$

where $G(r, t)$ is the convective velocity along r or simply the growth rate of the ice crystal such that

$$G = \frac{dr}{dt}. \tag{8}$$

Equation 6 is then

$$\frac{\partial n}{\partial t} + \frac{\partial}{\partial r}(Gn) + D - B + \nabla(\vec{V}_e n) = 0\,. \tag{9}$$

This is the number continuity equation in general form. Further simplifications can be made by applying physical knowledge of frazil and the conditions under which it evolves. In principle, eq 9 can be solved for n (crystal size distribution) if G, B and D are known functions, and the initial and boundary conditions of n are known. To uniquely define these parameters, the heat balance of the volume must be known. The basic equation governing the heat balance will be developed later.

Crystal moment equations

It is often of interest to know the distribution with crystal size of the number of crystals, the mass of crystals or surface area of the crystals. These can be uniquely determined if the distribution function is known. Let $n(r, t)$ be the distribution of the crystal population along the crystal size axis r at a time t. For convenience we assume that n is not dependent on any other coordinate and t is fixed; $n(r)$ is the population density of crystals of size r. By definition, the concentration of crystals of size r to $r+dr$ found in a unit volume is

$$dN = n(r)dr. \tag{10}$$

The units of n are (r^{-3}), (r^{-1}) or (r^{-4}). The total concentration of crystals is

$$N = \int_0^\infty n(r)dr. \tag{11}$$

The units of N are crystals per unit volume. The surface area of an individual crystal can be represented as

$$a(r) = K_a r^2 \tag{12}$$

where K_a is a shape factor relating area to size squared. For geometrically similar crystals the shape factor is independent of size. The total surface area per unit volume of suspension is

$$A_T = K_a \int_0^\infty r^2\, n(r)dr. \tag{13}$$

The weight of an individual crystal can be represented as

$$m(r) = \rho_i K_v r^3 \tag{14}$$

where K_v is a volumetric shape factor relating the volume to size cubed and ρ is the crystal density. The total mass of crystals per unit volume of suspension is

$$M_T = \rho_i K_v \int_0^\infty r^3\, n(r)dr. \tag{15}$$

Heat balance

In this section the general expression for the heat balance of the frazil ice-water system will be developed. This expression will be developed strictly for frazil crystals suspended in fresh water.

Consider a differential volume in which $\hat{\rho}_f$ is the mass concentration of water (grams of water per cubic centimetre of mixture) and $\hat{\rho}_i$ is the mass concentration of ice. The temperature of the water is T_f and the ice T_{ice}, then

$$C\frac{\partial}{\partial t}(\hat{\rho}_f T_f) + C_i\frac{\partial}{\partial t}(\hat{\rho}_i T_{ice}) + C\nabla(\hat{\rho}_f T_f \vec{V}_f) + C_i\nabla(\hat{\rho}_i T_{ice}\vec{V}_e) =$$

$$-\nabla k \nabla T_f + \hat{\rho}_f \upsilon \Phi + Q^* + L_{te}\left[\frac{\partial}{\partial t}\rho_i + \nabla\left(\rho_i \vec{V}_e\right)\right] \tag{16a}$$

where C = heat capacity of liquid water
C_i = heat capacity of ice
$\vec{V}_f$ = convective velocity of the fluid
k = thermal conductivity
υ = kinematic viscosity
Φ = dissipation function (viscous heating)
Q^* = net heat transfer from the mixture
L_{te} = latent heat of fusion of the ice at the equilibrium temperature of the mixture.

Several simplifications can be made to eq 16a. The first is to assume that $T_f \approx T_{ice}$, that is, the temperature of the ice is that of the water. While this cannot be strictly true (if it were there could

be no heat transfer between the ice and water), this assumption introduces only a very small error. The error is small as the temperatures of the ice and water are very close, usually within 0.1 C. Also the mass of ice is usually very small compared to the mass of water ($\leq 1\%$), so that to good approximation, $\dot{\rho}_f$ can be set equal to ρ_f, the density of water, and $\rho_f + \rho_i \sim \rho_f \sim \rho_f$. A second assumption is then $C_i \rho_i / C \rho_f \ll 1$. Additionally, heat conduction can be neglected and heat capacities and the latent heat can be considered constant because of the small variation in temperature. Therefore, based on the above assumptions, eq 16a can be rewritten

$$\frac{\partial T_f}{\partial t} + \nabla(\vec{V}_f T_f) = \frac{L}{C \rho_f} \left[\frac{\partial}{\partial t} \dot{\rho}_i + \nabla(\vec{V}_e \dot{\rho}_i) \right] + \frac{Q^*}{C \rho_f} + \frac{\upsilon \Phi}{C} . \tag{16b}$$

where L is the latent heat, which can be assumed to be a constant.

Parameters in the basic equations

The two basic equations are the crystal number continuity (eq 9), and the heat balance (eq 16b). The various parameters that appear in these two equations will now be discussed.

1. **G**–The growth rate of the major linear dimension of the crystals is a function of the heat transfer and the intrinsic kinematics of the ice crystal. In the *Ice Crystal Growth Rates* section it will be shown that G is effectively determined by the heat transfer rate. Thus, in general

$$G = \frac{h(r, \epsilon)}{\rho_i L} \theta$$

where h is the heat transfer coefficient and is a function of the crystal size r and the level of turbulence ϵ; θ is the supercooling of the mixture.

2. **D**–The death function can be set to zero for all signs of crystals. This is equivalent to assuming that there is no large-scale breakage of the crystals.

3. **B**–The birth function is determined by the rate of the sudden appearance of new crystals. New crystals can appear as a result of spontaneous nucleation, secondary nucleation and the introduction of crystals. The *Nucleation* section will show that spontaneous nucleation is not possible under frazil-forming conditions. Therefore B will be determined by the rate at which new crystals are introduced and the rate of secondary nucleation.

Let $\dot{N}_T$ be the rate of secondary nucleation. $\dot{N}_T$ is a function of the crystal distribution n, the turbulence dissipation rate ϵ, the supercooling of the mixture θ, and perhaps other parameters. Let $\dot{N}_I$ be the rate at which new crystals are introduced. We assume that new crystals are created and introduced at a size small enough that the radius of new crystals can be approximated as zero. Thus

$$B = [\dot{N}_T(\theta, n, \epsilon) + \dot{N}_I] \, \delta(r-0)$$

where $\delta(r-0)$ is the dirac delta function $[\delta(r = 0) = 1, \delta(r \neq 0) = 0]$.

4. $\dot{\rho}_i$–The mass of ice per unit volume of mixture can conveniently be determined using the moment equation

$$\dot{\rho}_i = \rho_i K_v \int_0^r r^3 \, n(r) \, dr .$$

5. Q^*, Φ–These functions are determined by the environment of the water body of interest, and, in particular, the meteorologic and hydraulic conditions. Φ, the dissipation function, will generally be quite small and under most circumstances can be set equal to zero with small error. Expressions to determine the value of these functions will not be developed in this report.

6. $\vec{V}_e$, $\vec{V}_f$ The convective velocity of the ice crystals and the fluid will generally be very similar.

The action of buoyancy and inertial forces on the ice crystals may cause the ice crystal velocity to differ from the fluid velocity if these forces become large compared to the fluid drag force.

Substituting the above expressions into eq 9 and 16b gives us

$$\frac{\partial n}{\partial t} + \frac{\theta}{\rho_i L}\frac{\partial}{\partial r}(hn) + \nabla(\vec{V}_e n) = (\dot{N}_T + \dot{N}_I)\,\delta(r-0)$$

$$\frac{\partial \theta}{\partial t} + \nabla(\vec{V}_f \theta) = \frac{L\rho_i K_v}{C\rho_f}\left|\frac{\partial}{\partial t}\int_0^{\infty} r^3 n\,dr + \nabla(\vec{V}_e \int_0^{\infty} r^3 n\,dr)\right| + \frac{Q^*}{C\rho_f}$$

where $n = n(x,y,z,r,t)$
$\theta = \theta(x,y,z,t)$
$h = h(r,\epsilon)$
$\vec{V}_e = \vec{V}_e(x,y,z,r,t)$
$\dot{N}_T = \dot{N}_T(\theta,\epsilon,n)$
$\vec{V}_f = \vec{V}_f(x,y,z,t)$
$Q^* = Q^*(x,y,z,t)$.

Writing the equations in this form emphasizes the dynamic way in which they interact. To determine θ and n uniquely, both equations must be solved simultaneously, and the boundary conditions and initial conditions of θ and n must be known. Difficulties arise because θ and n are dimensionally incompatible. In the *Ice Crystal Growth Rates* section expressions for h will be developed and in the *Nucleation* section expressions for $\dot{N}_T$ will be developed.

ICE CRYSTAL GROWTH RATES

Introduction

This section is a discussion of all the relevant factors that determine the growth rates of ice crystals suspended in turbulent flows. These factors include the morphology, the intrinsic kinetic growth rates and the heat transfer processes. The overall goal of this section is to determine the value of the parameter G that appears in the number continuity equation.

Morphology

A description of the morphology of ice is not simple. The various shapes of ice crystals appear to result from a complex interaction of the imposed heat transfer conditions and the intrinsic crystallography of ice. We know from observations that the dominant shape of ice crystals that grow at the supercooling levels found in turbulent water bodies is a flat disk. Virtually all field observations of frazil ice note that the crystals are disk shaped. It has been reported that ice crystals in the shape of six-pointed stars, hexagonal plates or spheres, and small pieces of dendritic ice all evolve into the disk shape in natural water bodies. Researchers have studied the morphology of large numbers of frazil ice crystals because of interest in desalination by freezing. The observations of Margolis (1969) indicate that the thickness of the frazil disk is $0.68r \pm 16.7\%$, where r is the major radius of the disk. Smith and Sarofim (1979) say that the maximum radius is approximately 0.8 mm for disk crystals produced in turbulent crystallizers.

Disk-shaped crystals have been studied in the laboratory by Kumai and Itagaki (1953), Arakawa (1954) and Williamson and Chalmers (1966). Arakawa's classic drawing of the growth of a disk crystal is shown in Figure 3. Arakawa created disk crystals by first growing dendritic ice crystals on the bottom of a container containing slightly supercooled water. He then scratched the crystals with the tip of a fine needle. Spherical ice particles with a diameter of about 10^{-2} mm formed and rose towards the surface. Two flat spots formed on the spherical particles' surface as they

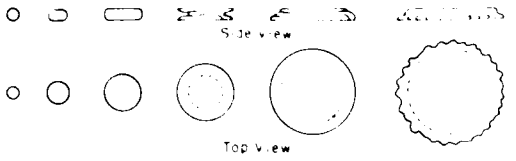

Figure 3. Frazil disks (after Arakawa 1954).

floated up, and further growth was lateral: the particles became disks. The crystals grew into disks with diameters of 0.5 to 3 mm and with diameter-to-thickness ratios of 5:1 to 100:1. Once the disks grew to a certain size they took on a notched look with many notch-shaped growths at the perimeter of the disk.

In a series of experiments, Williamson and Chalmers (1966) found that at supercooling levels of 0.2°C or less, ice grows into disk crystals. On increasing the supercooling level to 0.4°C, they found that the disk morphology became unstable and small protuberances appeared on the edge of the disks. The protuberances did not appear to show any preferred growth directions. At supercooling levels greater than approximately 0.6°C, the ice assumed the characteristic dendritic appearance shown by many snowflakes, and preferred growth directions developed. For supercooling greater than −1°C, preferred growth directions dominated the morphology and produced dendritic crystals with at least three generations of branches.

Researchers think that the disk shape taken by ice at low supercooling levels is the result of the anisotropic growth kinetics of ice. Ice has two growth axes and they are identifiable by their optical properties. The ice molecule is hexagonal. The hexagonal axis is the *c*-axis, and the three axes normal to the *c*-axis are the *a*-axes. The *a*-axes are all equivalent because the crystal is symmetrical about the *c*-axis. The plane that contains the *a*-axes is the basal plane, and the growth rate in it is tens of times faster than that parallel to the *c*-axis.

The disk shape of the ice crystal is subject to morphological instability. In natural water bodies this instability is observed as scalloped edges, dendritic growths, irregular protuberances, etc., on the perimeter of the crystals. Experiments have shown that the disk shape always becomes unstable if the supercooling is increased enough or if the diameter of the crystal becomes large enough. Instability is perhaps the mechanism that limits the maximum disk radius to 0.8 mm. The entire reason for the instability of the disk shape is not known, although it has been the subject of several investigations (Williamson and Chalmers 1966, Fujioka and Sekerka 1974). Williamson and Chalmers concluded that the instability of the disk shape depends on heat flow into the liquid, not crystallography. This conclusion seems correct, as the diameter at which the crystal becomes unstable varies between experiments.

Intrinsic kinetic growth rate

The mechanisms that determine the rate at which an ice crystal can grow are transport of water molecules to the crystal surface (for ice grown in the pure water this is not a consideration), their incorporation into the crystal surface and the transport of latent heat away from the surface. The incorporation of molecules is controlled by the crystallization or interface kinetics of ice and the heat transfer reflects the particular physical situation of the system under consideration. The interface kinetics of ice has been studied both theoretically and experimentally. As noted in the previous section, ice has two principal growth directions: within the basal plane (*a*-axis growth) and normal to the basal plane (*c*-axis growth). The interface kinetics of each growth direction appear to be different and each will be addressed separately.

The crystallization kinetics of ice can be viewed as part of the larger study of crystal growth from a melt, which has developed an extensive literature. In the interest of brevity, the interface kinetics will be divided into three simple possibilities, following the example of Fletcher (1970).

The first possibility is that of a perfectly smooth crystal face. Because of the lack of near neighbors, it is relatively difficult for molecules to become attached to such a surface. It is necessary for a stable "island" to nucleate on the surface before growth can begin. For this type of growth it can be shown that

$$G_k \approx \exp(-a/\theta_i) \tag{18}$$

where G_k is the kinetic growth velocity, a is a constant and θ_i is the supercooling at the interface. This type of growth is called surface nucleation.

Real crystal's surfaces are generally not perfectly smooth and may contain imperfections of various kinds. A dislocation imperfection allows the crystal surface to advance continuously. For this type of growth it can be shown that

$$G_K \simeq \theta_i^2. \tag{19}$$

This type is called growth by dislocation mechanisms.

A crystal surface may, under certain circumstances, be rough on a molecular scale. All crystals show a general tendency to become rough at large supercooling levels and it is relatively easy for molecules to become attached to a rough surface. The velocity of this type of growth can be shown to be

$$G_k \simeq \theta_i. \tag{20}$$

This type of growth is called continuous growth. The continuous growth mechanism may be affected by the curvature of the interface, especially if the radius of curvature is very small.

Measurements of growth velocity fall into two general classes: those in which free dendritic growth is measured and those which confine the growing ice in a tube that is placed in a bath of some other liquid. Both methods suffer from a disadvantage because the interface temperature can't be directly measured.

Measurements of the growth velocity in the direction normal to the basal plane were made by Hillig (1958) and Sperry (1965). In both cases the growing ice was confined to a capillary tube. Although the results are not in precise agreement, they suggest that ice grows in the c-axis direction by surface nucleation. Damaged crystals grew faster than undamaged crystals; they thought that damage to the interface provided the imperfections necessary for dislocation-type growth. They found that a minimum supercooling level was necessary before growth was observed—additional evidence of a surface nucleation mechanism.

Measurements of the growth velocity in the direction parallel to the basal plane have been made by a large number of investigators (Fletcher 1970, Hobbs 1974, Kallungal and Barduhn 1977). Fletcher describes the results of many investigators as showing rough qualitative agreement. All the measurements can be described by a relation of the form

$$G_k = a(\theta_i)^b. \tag{21}$$

Unfortunately, the value of the exponent b has been found to vary from 1.3 to 2.2, and measurements made at the same value of θ_i vary widely.

It is difficult to assess how accurately the data represent the interface kinetics and not complications of the heat transfer effects. The results were generally interpreted as implying a dislocation mechanism, but this interpretation has been criticized by Jackson et al. (1967). Kallungal and Barduhn (1977) state: "Interpreting growth rates in capillaries is a difficult and unrewarding task since the rates are as much dependent on the properties and physical dimensions of the capillary tube as the characteristics of ice and water." To resolve the question of a-axis growth rate, they made a number of measurements of free dendritic growth in both flowing and quiescent water. They found that at large impressed water velocities, heat transfer of the boundary layer type controlled the growth. No influence of interface kinetics was found to exist up to impressed velocities of 68 cm/s. They demonstrated that in quiescent water the growth direction with respect to gravity strongly affects the results. This they interpreted as evidence of heat transfer complications due to natural convection. The importance of natural convection to ice growth rates was also demonstrated by Gilpin (1976). The rest of the literature contains no consideration of natural convection heat transfer.

In summary, the different growth rates parallel to the basal plane and normal to the basal plane of an ice crystal are the result of differing interface kinetics. Growth in the *c*-axis probably proceeds by surface nucleation for perfect crystals and by a dislocation mechanism for damaged crystals. The interface kinetics of *a*-axis growth has not been completely defined; the mechanism is probably that of continuous growth. However, it appears that the kinetics are very fast and that for practical purposes the growth rate is totally controlled by the rate at which heat is transported away from the interface.

Combined effects of kinetics and heat transfer on the growth rates

The rate of growth of an ice crystal depends on two processes that take place in series - the attachment and rearrangement of water molecules on the crystal surface in accordance with the intrinsic kinetics, and the transport of the latent heat of fusion away from the crystal surface. Depending on the relative rates of these two processes, either could control the growth rate. Prediction of the growth rate involves determining how the separate processes interact and how the two can be combined to give an overall growth rate.

The growth rate will be modeled here as two processes in series, and the influence of the surface curvature will also be included. Let T_f be the bulk temperature of the supercooled liquid, and T_m be the equilibrium temperature of the ice-water mixture. For pure water, the equilibrium temperature will be 0°C. The overall supercooling level θ can be obtained as the sum of the three temperature differences representing the driving forces required to overcome the surface curvature, intrinsic crystallization and the heat transfer resistances:

$$\theta = T_m - T_f = (T_m - T_e) + (T_e - T_i) + (T_i - T_f) \tag{22}$$

where $(T_m - T_e)$ is the temperature difference required to overcome the surface curvature resistance, $(T_e - T_i)$ is required to overcome intrinsic kinetics resistance and $(T_i - T_f)$ is required to overcome the heat transfer resistances.

The surface curvature resistance is a function of the radius of curvature of the ice/water interface. The temperature needed to overcome this resistance can be estimated

$$T_e = T_m - \frac{2\gamma T_m}{\rho_i L r} \tag{23}$$

where γ = ice/water interfacial tension ($\gamma \simeq 22$ erg cm^{-2} [Fletcher 1970])

L = latent heat of fusion per gram of ice

r = radius of curvature

ρ_i = density of ice.

T_e can now be estimated as 3.9×10^{-6} cm °C/r. Therefore, if $r > \sim 10^{-3}$ cm (10 μm) then the curvature effect will be essentially negligible. We can assume that for the purposes of this study that this will always be the case. Therefore, eq 22 can be rewritten as

$$\theta = T_m - T_f = (T_m - T_i) + (T_i - T_f) \tag{24}$$

where $(T_m - T_i)$ is required to overcome the intrinsic kinetics resistance. Let q be the rate of heat transfer per unit surface area. Assuming a steady growth rate, we see that

$$q = a(T_m - T_i)^b = h(T_i - T_f) = \bar{h}(T_m - T_f) \tag{25}$$

where a and b are the crystallization kinetics coefficients, h is the heat transfer coefficient and $\bar{h}$ represents an overall transfer rate. We can make the crystallization kinetics linear as

$$a(T_m - T_i)^b = a' + a''(T_m - T_i) \tag{26}$$

and thus

$$q = \bar{h}(T_m - T_f) = \frac{h(T_m - T_f) + (ha'/a'')}{[1 + (h/a'')]}. \tag{27}$$

The growth rate along the a-axis determines the major linear dimension of the frazil disk. Therefore, it is the a-axis growth rate that appears in the number continuity equation as the function G. Kallungal and Barduhn (1977) measured a-axis growth rates and found no evidence of a rate limiting kinetic step. This implies that $a'' > h$. Thus

$$G = \frac{q}{\rho_i L} = \frac{h}{\rho_i L}(T_m - T_f). \tag{28}$$

The growth rate in the a-axis is strictly controlled by heat transfer. An expression for the heat transfer coefficient h will be determined in the next section.

Growth along the c-axis is much slower than a-axis growth for all sizes of crystals. This implies that c-axis growth is controlled by the intrinsic kinetics and thus $h > a''$. The c-axis growth rate does not appear in the number continuity equation. The latent heat released by growth along the c-axis may contribute somewhat to the overall heat balance; however, research has revealed that the latent heat released by c-axis growth is effectively negligible. Therefore, only the growth along the a-axis will be considered.

Heat transfer from ice crystals suspended in turbulent water

Introduction

In this section expressions for the rate of heat transfer from suspended ice crystals will be formulated. To determine the transfer ratio, it is necessary to describe the ambient velocity distributions of the fluid about the crystal. Frazil is created and develops only in water that is turbulent. Rivers and channels are inherently turbulent because of the instability of their bulk currents. Wind can make large water bodies become turbulent. Frazil is also created in crystallizers in which the water is made turbulent by impellers, turbines or other means. To describe the velocity distribution of the water surrounding the crystals requires knowledge of the properties and characteristics of turbulence. The first part of this section will be a very brief review of the Kolmogorov theory of locally isotropic turbulence. For further details the reader should examine the texts of Batchelor (1953), Hinze (1959) and Tennekes and Lumley (1972).

Analytical expressions for heat transfer have been developed for particles immersed in a stationary fluid, in a fluid moving with a uniform translational motion, and in a fluid whose velocity varies linearly with position (shear flow). These analytical expressions will be discussed later in this section.

If the ambient velocity about a suspended particle in turbulent water cannot be described in terms of these velocity distributions, an analytical expression may not be possible. In this case a more empirical expression is necessary. Frazil crystals are subject to gravitational and inertial forces which give them an additional translational motion relative to the fluid because the density of ice is different from that of water. The magnitude of this translational motion is determined in this section and its possible influence on the transfer rates is assessed. Also, as the ice crystals are not spherical, the influence of their disk shape on the transfer rates is determined. For the growth of frazil in fresh water, only the transfer of heat must be determined. The corresponding treatment and results for mass transfer from suspended particles are identical when expressed appropriately.

Fluid turbulence

The physical basis of the Kolmogorov theory of turbulence can be visualized as numerous interacting eddies of all possible scales. The very largest eddies originate directly from the instabilities of the mean bulk flow. The scale and orientation of these largest eddies are imposed by the geometry of the flow situation. In a stirred crystallizer the largest eddies are created by the impeller and are in scale with the impeller width these large eddies constitute the bulk flow. In a river or channel the size of the largest eddies are limited by the depth or width of the channel. In a large body of still water, in which the turbulence is generated by the shear stress of the wind, it is not possible to easily predict the scale of the large eddies, unless some nonhomogeneous feature, such as a thermocline, exists.

Energy is extracted from the large eddies through the inertial interaction of these eddies with smaller eddies. The amount of kinetic energy per unit mass in the large-scale eddies is proportional to u^2, where u is their velocity. This energy is assumed to be lost in a time proportional to ℓ/u, where ℓ is the length scale of the eddies. Thus, the rate at which energy is supplied from the large-scale eddies to the smaller eddies is $u^2 u/\ell = u^3/\ell$. This energy cascades through the spectrum of eddy sizes to the smallest eddies. As the eddy size becomes smaller, the geometric orientation of the large eddies is lost. The turbulence is isotropic when smaller eddies are randomly orientated. The energy cascade is not affected by the fluid viscosity until the smallest scales are reached, where this energy is dissipated by the viscosity. The dissipation rate must equal the rate at which energy is supplied to the small-scale eddies. Therefore, the dissipation rate ϵ can be defined as

$$\epsilon = u^3/\ell. \tag{29}$$

The scale at which viscous dissipation becomes important can be estimated if the fluid viscosity υ and ϵ are known. From these parameters it is possible to form a length scale η such that

$$\eta \sim (\upsilon^3/\epsilon)^{1/4}. \tag{30}$$

η is the dissipation length scale or the Kolmogorov scale.

For flows with a sufficiently high Reynolds number, if the spectrum of eddy sizes is normalized by the dissipation length scale, there is a universal character for the range of eddy sizes smaller than the large energy-containing eddies. This is the universal equilibrium range. The universal character of many different turbulent flows is shown in Figure 4, which is plotted to show the energy of eddies against the wave number of the eddies (reciprocal of wave length).

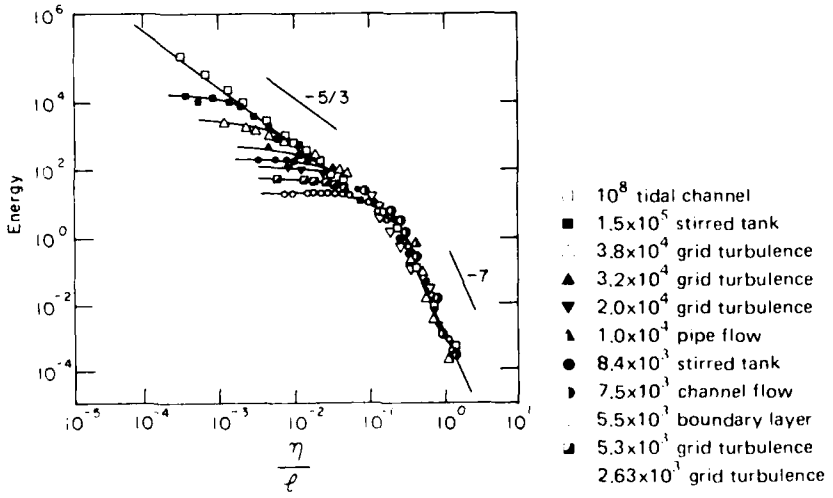

Figure 4. Universal turbulence spectra (after Wadia 1975).

The range of scales larger than the dissipation scale but smaller than the scale of the large energy-containing eddies is the inertial subrange. It is impossible to predict a priori the maximum scale at which the inertial subrange will begin. Within the inertial subrange the fluid viscosity has no effect and all energy dissipation results from the inertial interactions between eddies of different sizes. Therefore, the only scaling parameter available is ϵ, which can be interpreted as the rate (per unit mass of fluid) at which energy cascades through the spectrum of eddies sizes within the inertial subrange.

The range of scale that is smaller than the dissipation scale is the dissipation subrange. The fluid viscosity plays an important role in the subrange and acts quickly to dampen and dissipate the fluid motion. This small-scale motion automatically adjusts itself to the value of the viscosity and the rate of energy transfer.

Heat transfer from suspended particles

This discussion of heat transfer from force-free particles will concentrate on two kinds of flows: first, particles suspended in fluid with steady velocity distribution; second, particles suspended in turbulent fluid.

Linear velocity distributions. Probably the most basic situation that can be analyzed is that of an isothermal particle suspended in a motionless fluid, with no relative motion between the particle and the fluid. In this case the heat transfer rate is controlled purely by the rate at which heat can diffuse from the surface of the particle to the bulk of the fluid (Carslaw and Jaegar 1959). Whatever the particle shape, the steady distribution of temperature due to diffusion becomes spherically symmetric at large distances from the particle. At these distances the temperature distribution is the same as that which would be caused by continuous point sources of heat, emitting heat at the same rate as the actual particle.

It is convenient to define the nondimensional measure of the heat transfer rate or Nusselt number Nu as

$$\mathrm{Nu} = (hr/k) \tag{31}$$

where r is the major radius of the particle, k is the thermal conductivity of the fluid, and h is the heat transfer coefficient. For a spherical particle of radius r in a stationary fluid, the heat transfer is

$$4\pi r\, k(T_s - T_f) = 4\pi r^2\, h(T_s - T_f) \tag{32}$$

where T_s is the temperature at the particle surface and T_f is the bulk temperature of the fluid. Therefore

$$\mathrm{Nu}_0 = 1\ . \tag{33}$$

The method used to determine the transport rate from the particle suspended in a fluid moving with a steady uniform velocity will depend on the value of the Péclet number, defined as

$$\mathrm{Pe} = (V_f r/\alpha) \tag{34}$$

where V_f is the steady translational velocity and α is the thermal diffusivity of the fluid.

If the Péclet number is small ($\mathrm{Pe} < 1$), the transport from the particle surface is dominated by diffusion. The effect of the fluid motion is to modify the spherically symmetrical, steady-state distribution of temperature due to diffusion at large distances from the particles and to increase the transport rate. Because the influence of the fluid motion is only evident at large distances from the particle, the transport rate is relatively insensitive to the Reynolds number and the particular form of the ambient flow field.

The solution of the steady-state heat transport equation from a suspended particle at a small Péclet number belongs to the class of problems known as singular perturbation problems. The steady-state problem was solved by Acrivos and Taylor (1962) and Brenner (1963) by using "inner" and "outer" expansions of the temperature fields and matching these solutions in their common domain of validity. The inner solution held for the region near the particle in which diffusion was assumed to dominate. The outer solution held for the region far from the particle where convection was assumed to dominate. The solution for the transfer rate is

$$\frac{Nu - Nu_0}{Nu_0} = \frac{1}{2} Nu_0 Pe. \tag{35}$$

If the Péclet number is large ($Pe > 1$), the transport from the particle surface is dominated by convection. The gradients of temperature exist only in a small boundary layer near the particle, outside of which the temperature can be assumed to be uniform. The transfer rate at a large Péclet number is dependent on the form of the fluid motion near the particle and therefore the shape of the particle. A uniform translational motion that is linear with position corresponds to the conditions of Stokes flow. The expression for transfer from spherical particles in Stokes flow at large Péclet numbers has been determined by Levich (1962), Brian and Hales (1969) and Batchelor (1979). The solution of Batchelor is

$$Nu = Nu_0 + 0.624\, Pe^{1/3}. \tag{36}$$

The third and most general situation is that of a particle immersed in a fluid with a steady velocity distribution that varies linearly with position. This type of flow—shear flow—has not had the extensive analysis of the previous two flows. In general, a linear velocity distribution can be represented as

$$\vec{V_f} = \vec{S}_{ij} \vec{x_j} \tag{37}$$

where $\vec{x_j}$ is position and the tensor $\vec{S}_{ij}$ can be written

$$\vec{S}_{ij} = \vec{E} + \vec{\Omega} \tag{38}$$

where $\vec{E}$ represents the pure straining motion of the fluid and $\vec{\Omega}$ represents a solid body rotation of the fluid. The angular velocity of the solid body rotation is determined by the vorticity of the ambient flow. We can see that a $\vec{S}$ of any magnitude can be produced by an infinite number of combinations of $\vec{E}$ and $\vec{\Omega}$.

Which combinations of $\vec{E}$ and $\vec{\Omega}$ are relevant for determining the transfer rates from a suspended particle? Batchelor (1979) provided the answer. An axis of symmetry along the particle can be determined by resolving the components of vorticity along the principal axes of the rate of strain tensor $\vec{E}$. It is the strain rate E_w along this axis of symmetry that is largely responsible for determining the transfer rates from a particle. Transfer in all other directions will be suppressed by the rotation of the fluid.

For shear flows the Péclet number can be defined as

$$Pe = \frac{r^2 S}{\alpha} = \frac{r^2 |E_w|}{\alpha}. \tag{39}$$

For small Péclet numbers, Batchelor (1979) determined the transfer rate, to the first order, as

$$\frac{Nu - Nu_0}{Nu_0} = 0.40\, Nu_0\, Pe^{1/3}. \tag{40}$$

For large Péclet numbers, Batchelor (1979) determined the transfer rate, to first order, as

$$Nu = Nu_0 + 0.97\, Pe^{1/3}. \tag{41}$$

Nonlinear velocity distribution. Particles suspended in a fluid moving with a nonlinear velocity distribution (relative to the particle) are subject to all situations in which the Reynolds number is large or the fluid is turbulent. At a large Reynolds number the fluid boundary layer forms, wake separation occurs, the boundary layer becomes turbulent, etc. This is important to many industrial processes because they depend on the transfer of heat to or from an object around which a fluid is flowing. If the shape of the object is complex, the transfer rates must be determined empirically. If the shape of the object is simple, such as a single cylinder or sphere, the heat transfer rate can be determined from known correlations of heat transfer rates and the properties of the flow. The Frössling equation is a well known correlation that relates the heat transfer from a sphere to the Reynolds number and Prandtl number of a steady flow. This relation, which has been found to be accurate for Reynolds numbers between 1 and 10^5, is

$$Nu = Nu_0 + 0.42\ Re^{1/2}\ Pr^{1/3}. \tag{42}$$

Re is the Reynolds number defined as $Re = r\ V_t / v$. The Prandtl number is defined as v / α (kinematic viscosity/thermal diffusivity).

At this point, expressions for the transfer rate from particles suspended in a turbulent fluid will be determined. In a previous section the dissipative and inertial subranges of the turbulent spectrum were described. We will see that the ambient velocity distribution of the dissipative subrange can be described in terms of linear motion and the inertial subrange cannot; very different means of determining the transfer rates are required in each subrange. Therefore, these two subranges can be said to compose two regimes of heat transfer. Unfortunately, we cannot know beforehand which regime the frazil will be in, as the size of the crystals and level of turbulence may vary widely in natural water bodies.

Particles in turbulence—dissipative regime. If the crystal size is small relative to the Kolmogorov length scale, it is in the dissipative regime. In the dissipative regime the fluid eddies are strongly dampened and dissipated by the fluid viscosity. In effect, the crystal is smaller than the smallest scales of the turbulent eddies. It does not experience the turbulence as interacting eddies but rather as a fluid motion that varies linearly with position. The magnitude of S in the dissipative regime can be estimated as (Tennekes and Lumley 1972)

$$S \sim (\epsilon / v)^{1/2}. \tag{43}$$

The Reynolds number of the particle motion will be (assuming the particles experience only this shear)

$$Re = (r^2\ \epsilon^{1/2}) / v^{3/2} \tag{44}$$

and the Péclet number

$$Pe = (r^2\ \epsilon^{1/2}) / (\alpha\ v^{1/2}). \tag{45}$$

As $r < \eta$ in the dissipative region,

$$r < (v^3 / \epsilon)^{1/4}$$

and therefore

$$Re < 1.$$

For the Péclet number to equal unity, that is, $Pe = 1$,

$$r = (1/Pr^{1/2})\eta \tag{46}$$

where Pr is the Prandtl number. Therefore, when

$$r < (1/Pr^{1/2})\eta; \quad Pe < 1 \tag{47a}$$

$$r > (1/Pr^{1/2})\eta; \quad Pe > 1. \tag{47b}$$

In the analysis of mass transfer, usually the Prandtl number (or analogously for mass transfer, the Schmidt number) is much larger than 1. Therefore, the low Péclet case corresponds only to very small particles, usually much smaller than the range of interest. However, for heat transfer from frazil crystals, the Prandtl number is approximately 13, and the low Péclet case is relevant. It is interesting to note that there is only a narrow range in which $Pe > 1$ and $Re < 1$. As the particle size becomes large, r will approach the Kolmogorov scale, η, and the conditions of the dissipative regime will no longer be valid. However, data suggest (Batchelor 1980) that the flow distribution can be considered linear until $r \approx 10\eta$, which expands the large Péclet number range. In the interest of generality, then, the result for both the small and large Péclet cases will be given.

As noted, Batchelor identified E_w as the important component of the shear for determining the transfer rates. The average over time $<|E_w|>$ is a parameter of the turbulent fluid in which the particle is immersed and is independent of the properties of the particle. The small-scale properties of the turbulence, in particular, determine its value.

Batchelor (1980) showed that in locally homogeneous and isotropic turbulence

$$<|E_w|> = 0.18(\epsilon/\upsilon)^{1/2}. \tag{48}$$

Therefore, Batchelor's result for the heat transfer at a small Péclet number (eq 40) can be written

$$\frac{Nu - Nu_0}{Nu_0} = 0.17\, Nu_0 \left(\frac{r^2}{\alpha}\,\frac{\epsilon^{1/2}}{\upsilon^{1/2}}\right)^{1/2}. \tag{49}$$

The large Péclet number result of Batchelor (eq 41) can be written

$$Nu = Nu_0 + 0.55\left(\frac{r^2\,\epsilon^{1/2}}{\alpha\,\upsilon^{1/2}}\right)^{1/3}. \tag{50}$$

These results are for a particle immersed in a shear flow produced by the turbulence of the fluid. It is assumed that there are no inertial forces or buoyancy forces acting on the particle that would cause additional movement of it relative to the fluid.

Particles in turbulence–inertial regime. If the crystal size is large relative to the Kolmogorov length scale it is in the inertial regime. A number of theories of mass transfer in the inertial regime have been developed and abandoned by the chemical engineers. These are discussed by Wadia (1975). The cause of the difficulty is that the flow field in the vicinity of the crystal is complex and the transfer may proceed at many scales. The particle may interact with fluid eddies that are both larger and smaller than it is. The problem then becomes characterizing the ambient velocity distribution so as to accurately determine the heat transfer rate.

The ambient velocity can be characterized in many different ways, each corresponding to a different eddy size. It seems reasonable to assume, following Wadia (1975), that the predominant shear that the particle will experience will be produced by eddies closest to the particle that are of the same size as the particle. Eddies that are significantly larger than the particle will entrain both the particle and the fluid around it. Very small eddies relative to the particle size may enhance the overall transport by some mechanism of renewal of the boundary layer surrounding the particles.

but it is eddies of a size comparable to the size of the particle that will cause the most significant gradients near the crystal surface. Therefore, the shear can be estimated as (Levich 1962)

$$S \sim \epsilon^{1/3} r^{-2/3}. \tag{51}$$

This shear will not be linear with position. The Reynolds number of the particle motion will be

$$\mathrm{Re} = \frac{r^{4/3} \epsilon^{1/3}}{\upsilon} \tag{52}$$

and the Péclet number

$$\mathrm{Pe} = \frac{r^{4/3} \epsilon^{1/3}}{\alpha}. \tag{53}$$

As $r > \eta$ in the inertial regime

$$r > (\upsilon^3/\epsilon)^{1/4}$$

and therefore

$$\mathrm{Re} > 1$$

and the Péclet number is

$$\mathrm{Pe} > \mathrm{Pr}.$$

In the inertial subrange, a linear ambient velocity distribution does not exist. The Péclet number is large, therefore gradients of temperature will exist only in small boundary layers near the particles. Fluid boundary layers will also exist and, if the Reynolds number becomes large enough, they may become turbulent. This situation cannot be analyzed in terms of the linear velocity distributions described earlier. Therefore, to determine the heat transfer from the particles, the Frössling equation will be used, following the example of Wadia (1975). The mean square shear between two points separated by distance r in the inertial subrange can be estimated as (Batchelor 1953)

$$\sqrt{S^2} = 2.7(\epsilon^{1/3}) r^{-2/3}. \tag{54}$$

Substituting eq 54 and 52 into eq 42, we see that the Frössling equation becomes

$$\mathrm{Nu} = \mathrm{Nu}_0 + 0.70\left(\frac{r^{4/3} \epsilon^{1/3}}{\upsilon}\right)^{1/2} \mathrm{Pr}^{1/3}. \tag{55}$$

The applicability of this equation to the situation under discussion here remains open to question. This equation was derived for steady, nonturbulent flow, not shear flow. However, it is interesting to note that if the size of particle r is made into a number without dimensions by the Kolmogorov scale such that $r^* = r/\eta$, then the Frössling equation and the expression for the transfer rate with a large Péclet number and a general linear ambient velocity distribution reduce to

$$\mathrm{Nu} \approx (r^*)^{2/3} \mathrm{Pr}^{1/3} \tag{56}$$

and therefore have the same dependence on the independent parameters of size and the Prandtl number.

We write the Frössling equation using the characteristic shear of an eddy size equal to the particle size, so what can be determined about the influence of eddies larger and smaller than the particle size? Wadia (1975) calculated that eddies smaller than half the particle diameter account for less than 20% of its relative velocity. He determined that eddies larger than the particle diameter accounted for 65% of its relative motion, and eddies greater than five particle diameters were responsible for less than 12%. Kuboi et al. (1974) used high speed photography to study the motion of neutrally buoyant trace particles suspended in a turbulent stirred tank and in a flowing pipe. They found that the rms velocities of the particles were $2.0\,(\varepsilon r)^{1/3}$. This supports the theory that it is the eddies of size comparable to that of the particle that cause the fluid motion around the particle.

The small-scale motion, smaller than the size of the crystal, may enhance the heat transport from the crystal by penetrating the boundary layer around the crystal. It is difficult to quantify this process but this enhancement has been successfully accounted for (although empirically) by correlation of the turbulent intensity, α_T, of the fluid. α_T is defined as

$$\alpha_T = \sqrt{u^2} / \bar{V}_f \tag{57}$$

where $\sqrt{u^2}$ is the rms value of the velocity deviation from the mean velocity $\bar{V}_f$. The experiments of Lavender and Pei (1967) demonstrated that the Frössling equation could be written as

$$Nu = Nu_0 + 0.44 \alpha_T^a \, Re^{(1/2+a)} \, Pr^{1/3} \tag{58}$$

where a is an experimentally derived coefficient. They found that for

$$\alpha_T \, Re < 1000, \quad a \approx 0.035$$

and

$$\alpha_T \, Re > 1000, \quad a \approx 0.25$$

with the break occurring at the point at which the boundary layer becomes turbulent. Therefore, having $\alpha_T \, Re < 1000$ gives

$$Nu = Nu_0 + 0.70 \, \alpha^{0.035} \, Re^{0.535} \, Pr^{1/3} \tag{60a}$$

and having $\alpha_T \, Re > 1000$ gives

$$Nu = Nu_0 + 0.70 \, \alpha^{0.25} \, Re^{0.75} \, Pr^{1/3}. \tag{60b}$$

For $\alpha_T \, Re > 1000$, Nu is essentially independent of the crystal size. This range is where industrial crystallizers generally operate and the independence of the transfer processes and particle size is often seen. This observation has been generalized and is called McCabe's Law (see the *Steady-State Crystal Number Continuity Equation and Heat Balance in a MSMPR Crystallizer* section). This correspondence between theory and observation is encouraging.

Heat transfer from suspended ice crystals

At this point the heat transfer equations developed in the preceding section will be applied to ice crystals suspended in turbulent water. As the density of ice crystals is different from that of water $[(\rho_i - \rho_f/\rho_f) \approx 8\%]$, the crystals are subject to gravitational and inertial forces that give them a translational motion relative to the fluid. The magnitude of this translational motion must be

determined and its possible influence on the transfer rates assessed. Also, as the ice crystals are not spherical, the influence of their disk shape on the transfer rates must be determined.

Relative translational motion. Let the translational motion of a crystal relative to the fluid be U_R. If $rS/U_R \ll 1$, where S is the shear of the ambient fluid, then the transfer rates are determined primarily on the basis of the relative translational motion. The influence of the shear would be a second order or higher effect. If $rS/U_R \gg 1$, then the transfer rates are determined primarily on the basis of the shear of the ambient fluid. When $rS/U_R \approx 1$, Wadia (1975) assumed that an effective crystal velocity, $U_{R\,eff}$, such that

$$U_{R\,eff} \simeq [(rS)^2 + U_R^2]^{1/2} \tag{61}$$

could be used to calculate the transfer rate. The work of Batchelor (1979, 1980) supports this means of combining the velocity due to shear and that due to translational motion in estimating transfer rates.

Inertial forces. The relative motion due to the inertia of ice crystals will now be determined. A force balance on a crystal can be written as

$$K_v r^3 \rho_i \frac{d\vec{V}_e}{dt} = F_D + K_v r^3 \rho_f \frac{d\vec{V}_f}{dt} + \rho_f K_v r^3 \left(\frac{d\vec{V}_f}{dt} - \frac{d\vec{V}_e}{dt}\right) X \tag{62}$$

where K_v = volumetric shape factor ($K_v r^3$ = volume of crystal)
$\vec{V}_f$ = velocity of the fluid
$\vec{V}_e$ = velocity of the crystal
ρ_i = density of the crystal
ρ_f = density of the fluid
X = added mass.

We will assume that 1) gravity effects are negligible (they will be analyzed separately), 2) the density of crystals is small enough so that the fluid properties are essentially uninfluenced by the presence of the crystals, 3) all the elements of an eddy are accelerated identically, 4) the Basset term can be ignored, and 5) the fluid turbulence is statistically steady. Now let

$$\vec{A}_f = (d\vec{V}_f/dt) \tag{63a}$$

$$\vec{A}_R = (d\vec{V}_f/dt) - (d\vec{V}_e/dt) \tag{63b}$$

$$\vec{U}_R = \vec{V}_f - \vec{V}_e \tag{63c}$$

then

$$\rho_i K_v r^3 A_R = (\rho_i - \rho_f) K_v r^3 A_f - A_R K_v r^3 \rho_f X - F_D \tag{64}$$

as the vectors $\vec{A}_f$ and $\vec{A}_R$ are parallel.

To proceed from this point, the size of the crystal relative to the scale of the turbulence must be known.

If the crystal is in the dissipative range, then $r < \eta$ and the drag force can be estimated using Stokes Law

$$C_D = 12/\mathrm{Re}. \tag{65}$$

where C_D is the drag coefficient. Thus

$$\frac{K_v r^2}{6\pi\upsilon}\left|\left(\frac{\rho_i+\rho_f X}{\rho_i}\right)A_R-\left(\frac{\rho_i-\rho_f}{\rho_f}\right)A_f\right| = -U_R. \tag{66}$$

The relative acceleration and the fluid acceleration can be estimated in the following manner

$$A_f \approx u^*/T^* \tag{67}$$

where T^* is the characteristic time of the eddy of interest and u^* the characteristic velocity. As $r < \eta$ these quantities are estimated at the scale of η. Thus

$$A_f \approx \frac{(\epsilon\upsilon)^{1/4}}{(\upsilon/\epsilon)^{1/2}} = (\epsilon^3/\upsilon)^{1/4} \tag{68}$$

and

$$A_R = (U_R/T^*) = U_R(\epsilon/\upsilon)^{1/2}. \tag{69}$$

Substituting into eq 66 and solving for U_R, we find

$$U_R = \frac{(K_v r^2/6\pi\upsilon)\,[(\rho_i-\rho_f)/\rho_f]\,(\epsilon^3/\upsilon)^{1/4}}{(K_v r^2/6\pi\upsilon)\,[(\rho_i+\rho_f X)/\rho_f]\,(\epsilon/\upsilon)^{1/2}+1}. \tag{70}$$

Now the magnitude of the relevant shear rate can be estimated as

$$S = 0.18(\epsilon/\upsilon)^{1/2} \tag{71}$$

and the relative magnitudes of U_R and S can be estimated as

$$\frac{rS}{U_R} = \frac{(0.18K_v/6\pi)\,[(\rho_i+\rho_f X)/\rho_f]\,(r/\eta)^2+1}{(K_v/6\pi)\,[(\rho_i-\rho_f)/\rho_f](r/\eta)} \tag{72}$$

and it can be seen that if $r < \eta$

$$\frac{rS}{U_R} > 1 \tag{73}$$

where U_R is the relative translational motion produced by the inertial forces on the crystal.

The inertial force on crystals in the inertial regime will now be determined following the example of Levich (1962) and Wadia (1975). Starting with eq 64, we can estimate the relative acceleration between the crystal and the fluid as

$$A_R \approx U_R/T^* \tag{74}$$

where

$$T^* \approx \ell/U_R \tag{75}$$

and ℓ is the characteristic eddy length scale. Thus

$$A_R \approx U_R^2/\ell. \tag{76}$$

To characterize the velocity of the fluid, only the size of the eddy ℓ and the dissipation rate ϵ are available. Therefore

$$u^* \approx (\epsilon \ell) \tag{77}$$

and

$$A_f \approx u^*/T^* \tag{78}$$

where

$$T^* \approx \ell/u^*. \tag{79}$$

Thus

$$A_f \approx (u^{*2}\, T^*) = \epsilon^{2/3} \ell^{-1/3}. \tag{80}$$

F_D can be written

$$F_D = (C_D \pi/2) r^2\ \rho_f U_R^2 \tag{81}$$

then

$$U_R^2 = \frac{(\rho_i - \rho_f) K_v r^3 (\epsilon \ell)^{2/3}}{\rho_i K_v r^3 + \rho_f K_v r^3 X + (C_D/2)\pi r^2 \rho_f \ell}. \tag{82}$$

We can see that U_R is a function of ℓ. At a certain value of $\ell = \ell^*$, the relative velocity has a maximum value $U_{R_{max}}$. ℓ^* can be determined such that

$$\partial U_R/\partial \ell = 0. \tag{83}$$

ℓ^* is then

$$\ell^* = \frac{2(\rho_i K_v r^3 + \rho_f K_v r^3 X)}{(C_D/2)\pi r^2 \rho_f}. \tag{84}$$

Substituting into eq 82, we find

$$U_{R_{max}} = \frac{2}{3^{5/6}} \left(\frac{(\rho_i - \rho_f)}{(\rho_i + \rho_f X)^{1/3} (C_D \rho_f)^{2/3}} \right)^{1/2} (\epsilon r)^{1/3}. \tag{85}$$

As Levich (1962) found, the numerical coefficient of eq 85 probably has no great significance. It is provided to indicate the absence of large numerical coefficients.

We recall that in the inertial regime $rS = 2.7(\epsilon r)^{1/3}$; thus

$$\frac{rS}{U_{R_{max}}} \approx \left(\frac{(\rho_i + \rho_f X)^{1/3} (C_D \rho_f)^{2/3}}{(\rho_i - \rho_f)} \right)^{1/2} \tag{86}$$

and as $12 < C_D < 1.1$ and $(\rho_i - \rho_f) = 0.08$, we can see that when $r > \eta$

$$(rS/U_{R_{max}}) > 1 \tag{87}$$

where $U_{R_{max}}$ is the maximum relative translational motion produced by the inertial forces on the crystal.

We can conclude, therefore, that to a good approximation the inertial force can be ignored in determining the transfer rates from suspended ice crystals.

Gravity forces. The relative translational motion due to the force of gravity can be estimated by equating the drag force and the gravity force:

$$\frac{\rho_f - \rho_i}{\rho_f} K_v r^3 g = \frac{1}{2} \pi r^2 C_D \rho_f U_t^2 \tag{88}$$

where K_v is the volumetric shape factor, U_t is the terminal rise velocity of a crystal, and C_D is the drag coefficient. The drag coefficient of a disk whose major radius is perpendicular to the flow is a well known function of the Reynolds number and is available in many texts. Experimental observation has shown that disks under the influence of gravity do not always move steadily. At the higher Reynolds numbers, they also oscillate, glide and tumble. Each of these motions influences the drag coefficient. Turbulence also influences the drag coefficient in a complex manner. In general, these influences will all tend to increase the drag on the disks slightly. In Figure 5 the terminal rise velocity is plotted as a function of the major radius. The velocity was estimated by assuming that the disk rises steadily with its axis perpendicular to the vertical. This may be an overestimation of the rise velocity.

In the Stokes range of $r < 0.03$ cm

$$U_t = 0.08(g' \upsilon^{-1} r^2). \tag{89}$$

In the intermediate range of 0.3 cm $< r <$ 0.14 cm

$$U_t = 0.16(g'^{0.715} \upsilon^{-0.428} r^{1.14}) \tag{90}$$

and in the fully turbulent range $r > 0.14$ cm

$$U_t = 2^{-1.2} (g' r)^{1.2} \tag{91}$$

where g' is the reduced gravity ($g' = 2[(\rho_f - \rho_i)/\rho_f][gK_v/\pi]$). To compare the shear motion and the relative translational motion due to gravity, several assumptions will be made that are based upon physical knowledge of frazil and the likely sizes of the frazil crystals.

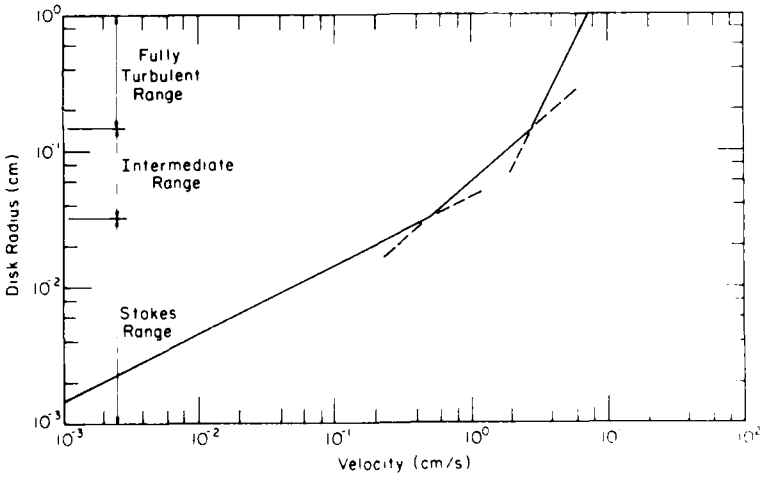

Figure 5. Terminal rise velocity of frazil disks.

We will assume that, if the ice crystal is in the Stokes range, that is $r < 0.03$, then it will also be in the dissipative regime. Then

$$\frac{rS}{U_t} = \frac{(\epsilon \upsilon)^{1/2}}{0.08 g' r} \tag{92}$$

and using the best estimate for υ and g', we see that

$$\frac{rS}{U_t} = \frac{0.02\,\epsilon^{1/2}}{r}, \qquad r < 0.03 \text{ cm}.$$

For the intermediate range, the crystal may be in either the dissipative or inertial regime. In the dissipative regime

$$\frac{rS}{U_t} = \frac{0.03\,\epsilon^{1/2}}{r^{0.14}}, \qquad 0.03 \text{ cm} < r < 0.14 \text{ cm} \tag{93}$$

and in the intertial regime

$$\frac{rS}{U_t} = \frac{0.11\,\epsilon^{1/2}}{r^{0.81}}, \qquad 0.03 \text{ cm} < r < 0.14 \text{ cm}. \tag{94}$$

The fully turbulent range corresponds to particles with radius larger than 0.14 cm. This is very large for a frazil disk; very few frazil crystals have been recorded larger than this size. Therefore, this range will not be considered further.

Given the maximum sizes of disks in the Stokes range and the intermediate range, ϵ need only be slightly larger than 1 for the shear velocity to dominate. This value of 1 corresponds to a relatively small level of turbulence. In most situations it will be possible to effectively ignore the translational motion induced by gravity in determining the heat transfer.

Heat transfer from disks. Up to this point, the heat transfer relationships have been developed for spheres. The influence of the nonspherical shape of ice crystals must be assessed.

The heat transfer from a disk in a stagnant fluid has been determined by Wadia (1975) and many others. Wadia demonstrated that if the major dimension of the disk was defined as $(A_s/4\pi)^{1/2} = \bar{r}$, where A_s is the surface area of the disk, then for a disk with aspect ratio 0.34,

$$\mathrm{Nu}_{\mathrm{DISK}} = (h\bar{r}/k) = 1. \tag{95}$$

The heat transfer from the edge and face of the disk can be represented as

$$\mathrm{Nu}_{\mathrm{EDGE}} = (h r_e/k) = 1$$

$$\mathrm{Nu}_{\mathrm{FACE}} = (h r_f/k) = 1$$

where r_e is one half the thickness of the disk and r_f is the radius of the face of the disk. Noting that $\bar{r} = 0.92r$, $r_e = 0.34r$, and $r_f = r$, we find

$$\mathrm{Nu}_{\mathrm{DISK}} = (hr/k) = 1.1$$

$$\mathrm{Nu}_{\mathrm{EDGE}} = (hr/k) = 2.94$$

$$\mathrm{Nu}_{\mathrm{FACE}} = (hr/k) = 1.0.$$

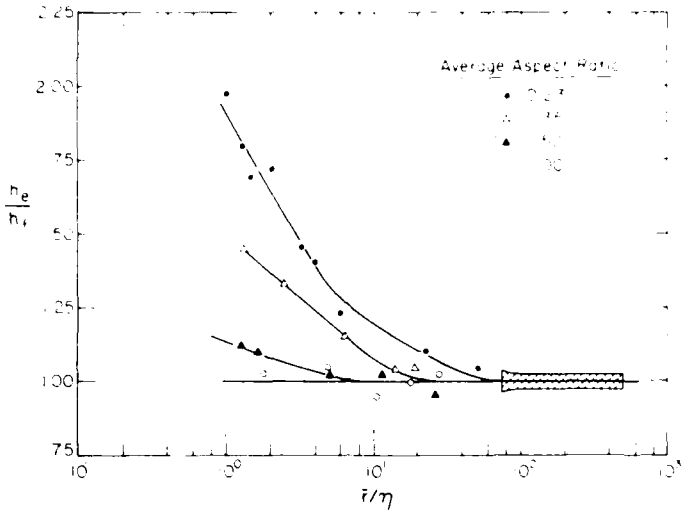

Figure 6. Edge vs face transfer (after Wadia 1975).

The heat transfer rate is much larger for the edge than the face of a disk. A general way of expressing this is

$$\mathrm{Nu} = (h\dot{r}/k) = 1 \tag{96}$$

where $\dot{r} = r_e, r_f, \bar{r}$.

If the crystals are in a turbulent fluid and are small enough such that $r < \eta(\mathrm{Pr})^{1/2}$, they are in the small Péclet number range where the heat transfer is dominated by diffusion. At small Péclet numbers the heat transfer rate is insensitive to the shape of the particle, as noted earlier. Therefore the disk shape will not influence the heat transfer to first order in this range. If the crystals are large enough such that $r > \eta$, then the Frössling equation, which was developed specifically for spheres, is applicable. To investigate the influence of the disk shape on the heat transfer rates predicted by the Frössling equation, Wadia (1975) conducted a series of experiments in which he measured the transport from disks of various aspect ratios. The results are shown in Figure 6. Wadia presented his results as the ratio of the measured heat transfer coefficient of the disk edge h_e to the heat transfer coefficient of the disk face h_f. The ratios are plotted against the nondimensionalized values of $\bar{r}/\eta$.

From his results, two trends can be observed. At low levels of $\bar{r}/\eta$, the ratio h_e/h_f increases rapidly as the aspect ratio (thickness/face diameter) departs from unity. Wadia's explanation of this result was that the local shear of the fluid was higher near the edge of the disk than on the face. For a fixed aspect ratio, as $\bar{r}$ is increased the h_e/h_f ratio decreases, approaching a value of 1 asymptotically. Wadia speculated that as the face dimension is larger than the edge dimension, the face of the disk can respond to a larger wave-number range of the small eddies, which can enhance surface renewal of the disk boundary layer. It is at the larger values of $\bar{r}$ that turbulent intensity plays a major role in influencing transport. Therefore, the effect of the turbulent intensity would be to enhance h_f more than it would h_e. At the large values of $\bar{r}$, the effects of higher local shear at the edges increasing h_e and the turbulent intensity enhancement of h_f would become of comparable magnitude, causing the ratio of h_e/h_f to approach unity.

From these results it is a direct step to determine a general correlation for the heat transport from a disk by use of the usual dimensional groups of the modified Frössling equation, but with r_e and r_f as the characteristic length scales. Wadia determined such a general correlation. He found that the results for all aspect ratios ($0.23 \leq x \leq 1.0$) are well correlated by a single line. This line is almost parallel to the sphere correlation line but slightly higher on average.

Wadia's conclusion is that for low aspect disks, the overall transfer coefficients, based on a mean surface area equivalent radius [$\bar{r} = (A_s/4\pi)^{1/2}$] are 10% higher than for spheres. And if the radius of the face and the edge thickness are used as the characteristic length dimensions for the face and edge, respectively, the results in dimensionless form agree well with those for the overall transport from a disk.

Summary

The Nusselt number for heat transfer from suspended particles is shown in Figure 7. The Nusselt number is calculated using the properties of water at 0°C, and a turbulent intensity of 0.2 is assumed. The heat transfer from spheres and disks is shown. The relevant size of the particle has been nondimensionalized by the dissipative scale η. Also shown are the heat transfer rates that would occur from a particle at its terminal velocity under the influence of gravity.

A method of determining the Nusselt number that provides an intuitively easier means of seeing the relative value of the actual heat transfer coefficient is as follows. Let Nu_T be the turbulent Nusselt number defined as

$$Nu_T = \frac{h\eta}{k} = \frac{h}{k}\left(\frac{\upsilon^3}{\epsilon}\right)^{1/4}.$$

Let $m^* = \hat{r}/\eta$ where $\hat{r} = \bar{r}, r_e, r_f$, or r (radius of a sphere). The heat transfer relationships are then:

for $m^* < 1/(\mathrm{Pr})^{1/2}$

$$Nu_T = (1/m^*) + 0.17\,\mathrm{Pr}^{1/2}$$

for $1/(\mathrm{Pr})^{1/2} < m^* < \approx 10$

$$Nu_T = [(1/m^*) + 0.55(\mathrm{Pr}/m^*)^{1/3}]$$

for $m^* > 1$, with a low intensity $\alpha_T m^{*4/3} < 1000$

$$Nu_T = [(1/m^*) + 0.70\alpha_T^{0.035}(\mathrm{Pr}/m^*)^{1/3}]\,\beta$$

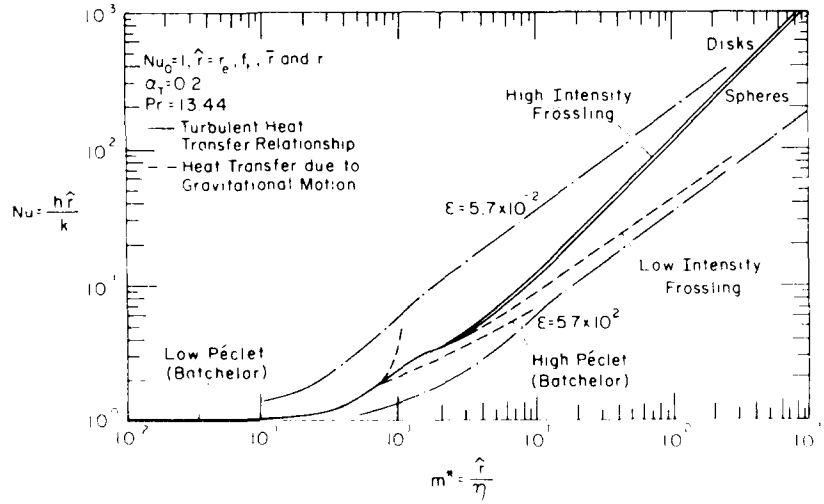

Figure 7. Nondimensional heat transfer correlation.

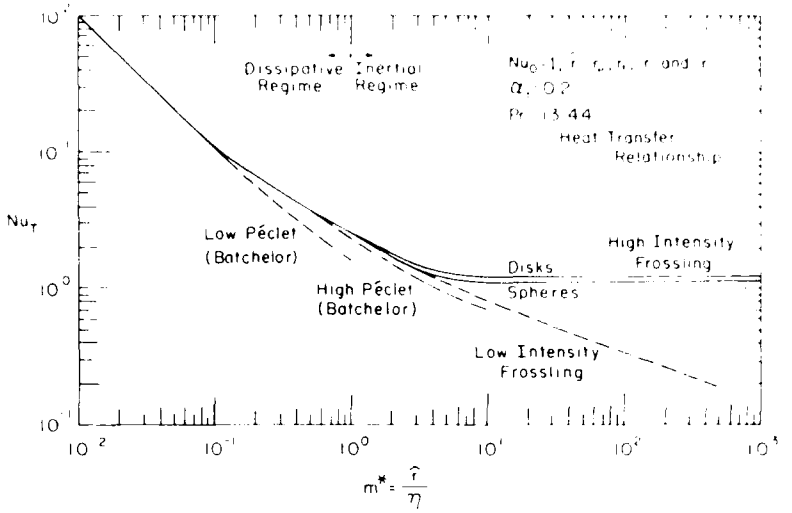

Figure 8. Nondimensional heat transfer correlation based on a turbulent Nusselt number.

for $m^* > 1$, with a high intensity $\alpha_T m^{*4/3} > 1000$

$$Nu_T = [(1/m^*) + 0.70\alpha_T^{0.25} Pr^{1/3}]\beta$$

where $\beta = 1.0$ for a sphere and 1.1 for a disk. These Nusselt number relationships are shown in Figure 8.

NUCLEATION

Initial nucleation

The initiation of the transformation of a substance from a less stable to a more stable phase is called nucleation. When the temperature of water is below the freezing point, the water is supercooled or undercooled, and it is less thermodynamically stable than water that is ice. The nucleation of supercooled water is the necessary first step in the formation of ice.

Researchers have thought that frazil ice may form by three types of nucleation: homogeneous nucleation, heterogeneous nucleation and secondary nucleation. Nucleation in an absolutely pure liquid is homogeneous nucleation. Nucleation that results from the presence of foreign particles is heterogeneous nucleation. Secondary nucleation results irrespective of its mechanism, only because of the presence of ice crystals in the supercooled liquid.

The importance of secondary nucleation to frazil ice formation has long been recognized (Altberg 1936). It is begging the question, however, to use secondary nucleation as the entire explanation for existence of frazil ice. Undoubtably, secondary nucleation plays the major role in increasing the total numbers of frazil crystals; it will be discussed later. The object here is to discuss the source of the original frazil crystals. The original crystals added to industrial crystallizers to begin secondary nucleation are called seed crystals. Are seed crystals necessary to start the formation of frazil ice in natural water bodies? If so, where and how do they originate?

Until fairly recently, researchers didn't think that seed crystals were necessary. At first it was thought that there was spontaneous homogeneous nucleation (Barnes 1928). It is well known today that there is no spontaneous nucleation in pure water unless the water is supercooled to approximately -38 °C, a temperature never found in any water body. Heterogeneous nucleation was next offered as the mechanism (Altberg 1936), and the experiments of Dorsey (1948) lent strong

support to this idea. Dorsey demonstrated that ice was nucleated by "motes" in the supercooled water. He defined motes as freely suspended particles of every kind and more generally as particular points of roughness in any solid boundary that touched the supercooled fluid. Schaefer (1950) reported seeing motes in the frazil crystals he grew in trays.

The chemical and physical characteristics of the motes such as shape, polarity and lattice mismatch between the motes and ice crystals are important in determining their effectiveness in nucleating ice. Dorsey demonstrated that once the temperature at which a sample of water froze spontaneously was determined (or more accurately, the temperature at which the motes contained in the sample caused nucleation), the water possessed complete thermal stability throughout the range of supercooling above that temperature. He found that samples of water could be supercooled to within 1°C of their predicted nucleation temperature and remain there for an indefinite time without freezing. However, if the temperature was lowered the 1°C, the sample would freeze. Any solid substance can be characterized by the minimum supercooling at which it will nucleate ice. A list of the nucleating temperatures associated with many substances, organic and inorganic, is provided by Hobbs (1974). The weakness of the heterogeneous theory is revealed by such a list. There are no known substances that will nucleate ice at the small levels of supercooling measured in natural water bodies. Piotrovich (1956) is credited with first pointing this out.

It is not possible to state categorically that a substance that can nucleate ice at the levels of supercooling measured in natural water bodies (less than 1°C) does not exist, only that none has been found. Such a substance was not present in the water samples tested by Osterkamp and Gilfillian (1975), which were taken from a stream that was producing frazil. The samples were cooled until they spontaneously froze. The range of temperature at freezing was −4.9 to −13.9 °C. The supercooling of the stream that the samples were taken from was less than 1°C. That the samples froze over a range of temperatures can be explained by assuming a random distribution of motes between the samples and by assuming that many different types of motes were present in the stream water. There were no substances contained in the samples that could effectively cause nucleation at the supercooling level known to exist in the stream. This is consistent with the experimental results of Dorsey (1948), Margolis (1969), Kane (1971), Evans (1973), Woltz (1975), Muller (1978), and others. This suggests that heterogeneous nucleation cannot be the mechanism responsible for the initial formation of the frazil crystals.

To remedy this weakness in the theory of heterogeneous nucleation, Michel (1971) has proposed the existence of a thin layer of very supercooled water immediately at the air/water interface. The supercooling of this layer would be sufficient to cause heterogeneous nucleation, somewhere in the range of 4.5°C. It is well known that a temperature gradient does exist at the surface of cooling water bodies (Paulson and Simpson 1981). However, in any water body containing the slightest degree of turbulence, it does not seem likely that the surface could be substantially colder than the bulk of the water.

Observations of frazil formation indicate that the first frazil crystals are often seen near the water's surface (Schaefer 1950, Arden and Wigle 1972). However, measurements of the surface supercooling level by thermometers (Arden and Wigle 1972) and radiation thermometers (Osterkamp and Gilfillian 1975) failed to measure any supercooling level beyond a few tenths of a degree more than that of the bulk temperature. Osterkamp (1977) summarized the available data and concluded that spontaneous heterogeneous nucleation in a thin supercooled surface layer of water cannot explain frazil ice nucleation. He also added that the possibility of heterogeneous nucleation existed only for very calm water surfaces such as on a puddle, pond or lake, but that the resulting ice form would be sheet ice rather than frazil ice.

All the available data indicate that spontaneous nucleation of ice is not possible in natural water bodies that are producing frazil; therefore, seed crystals are necessary. The seed crystals may come from outside the water body or from ice already in the water body. There are many situations where frazil ice has been observed in waters in which ice had not existed previously or where the ice was far from the zone producing frazil. Osterkamp (1977) proposed a mass exchange across the

air/water interface as the mechanism providing the seed crystals in these cases. The seed crystals are ice crystals that have a variety of origins. Water that originated in the water body and was introduced into the air by bubble bursting, splashing, windspray, evaporation, etc., can freeze and return in the form of ice crystals. It is interesting to note that often minimum air temperatures of -9 to -8 C are reported as necessary for the production of frazil. These temperatures correspond to the minimum temperatures at which spontaneous heterogeneous nucleation could be expected in water particles suspended in air. Ice particles that originated at some distances from the water body, such as snow, frost, ice particles from trees, shrubs, etc., could be effective seed crystals. Very cold soil particles and cold organic materials at temperatures less than the supercooling level necessary to cause spontaneous nucleation can also be introduced across the air/water interface and may serve to nucleate ice, although their effectiveness is not known.

In summary, the formation of frazil is started by the introduction of seed crystals into supercooled water. The mass exchange at the air/water interface proposed by Osterkamp (1977) is the most probable mechanism by which the seed crystals are introduced. The origin of the seed crystals and the rate at which they are introduced will depend on the local environmental conditions. The mass exchange mechanism provides a reasonable explanation for the observation of ice crystals at the water's surface at the start of frazil formation. This mechanism cannot explain the existence of all frazil crystals, however. The number of ice crystals increases rapidly when a crystal is introduced into turbulent supercooled water in which spontaneous nucleation is not possible. This increase in the number of crystals occurs only because of the presence of the original seed crystal secondary nucleation. Therefore, to determine the rate of increase of frazil ice crystals, the rate of introduction of new crystals and the rate of secondary nucleation must be known. The relative magnitude of these rates will depend on the local environment; however, the rate of secondary nucleation is probably much greater than the rate of introduction.

Secondary nucleation

Introduction

The processes that govern the rates of secondary nucleation are poorly understood. However, a partial modeling of the kinetics of secondary nucleation is possible based on the work of Evans et al. (1974a, b) who demonstrated that for ice the production rate of potential nuclei of new crystals and their removal from the parent crystals could be uncoupled. The most widely accepted source of the potential nuclei is surface irregularities that are sheared from the surface of the parent crystals (microattrition). Two general mechanisms of removal of the nuclei from the surface of the parent crystals have been suggested: collisions of the crystals with hard surfaces (including other crystals) and fluid shear. If the rate of secondary nucleation is limited by the production rate of potential nuclei, increases in the number of collisions of an individual crystal will not increase the production of new crystals. If the rate of secondary nucleation is removal-limited, however, the parent crystals will produce the same number of new nuclei each collision, independent of the crystal's time history. From their experimental work, Evans et al. (1974a, b) concluded that the secondary nucleation of ice was limited by the rate at which potential nuclei were removed from the crystal surface. Therefore, it was possible to determine the overall nucleation rate $\dot{N}_T$, with two or more mechanisms of removal, as the linear sum of the actual nucleation rate attributable to each mechanism of removal ($\dot{N}_i$),

$$\dot{N}_T = \dot{N}_1 + \dot{N}_2 + \ldots \dot{N}_i. \tag{97}$$

Based on the work of Clontz and McCabe (1972), Garabedian and Strickland-Constable (1972), Evans et al. (1974a, b), Woltz (1975) and others, we will assume that the removal of potential nuclei is caused solely by the shear produced during collisions of the parent crystals. The nucleation rate of each mechanism of collision can be expressed as the product of three functions (Botsaris 1976)

$$\dot{N}_T = (\dot{E}_t)(F_1)(F_2) \tag{98}$$

where $\dot{E}_t$ = rate of energy transfer to crystals by collision
F_1 = number of particles generated per unit of collision energy
F_2 = fraction of particles surviving to become nuclei

At this time the values of F_1 and F_2 must be determined empirically. Therefore, to simplify matters let F_1 and F_2 be combined and eq 98 be rewritten as

$$\dot{N}_T = \dot{E}_t S_N \tag{99}$$

where $S_N = (F_1)(F_2)$.

We expect that S_N is a function of all the parameters that govern the surface morphology and the crystal growth, including supercooling θ, impurity concentration C_I, turbulence level ϵ, etc. The total nucleation rate can be expressed as

$$\dot{N}_T = S_N(\theta, \epsilon, C_I, \text{etc.})(\dot{E}_{t1} + \dot{E}_{t2} + \dot{E}_{t3} \ldots). \tag{100}$$

The next parts of this section will focus on determining the rate of energy transfer for each mechanism of collision. Two general classes of crystal collisions can be identified: collisions between crystals in suspensions (crystal-crystal collisions) and collisions between crystals and external boundaries (crystal-boundary collisions).

We will assume that the nuclei produced by collisions are effectively at zero size. Therefore, the internal coordinate of the parent crystal remains unchanged during a collision. We also assume that large scale breakage of crystals, which has not been observed in natural water bodies or agitated crystallizers, does not happen during a collision.

Crystal-crystal collisions

We will assume all crystal-crystal collisions to be between two crystals only. Three types of collisions between crystals can be identified:

1. Collisions from the crystals moving with the fluid. These collisions are caused by spatial variations in the fluid motion.
2. Collisions from the crystals moving relative to the fluid. These are collisions caused by the crystals' inertia. It was shown in the *Ice Crystal Growth Rates* section that the velocity of the crystal caused by inertia forces was always much less than the velocity determined by the shear rate. Therefore, collisions caused by inertia will not be considered further.
3. Collisions caused by buoyancy.

Note that only collision type 1 will cause collisions between crystals of similar size.

The rate of energy transfer to the crystals by collision can be determined following the method of Evans et al. (1974b). $\dot{E}_t$ is the product of the collision energy $E(r_1, r_2)$ and the frequency of collision $q(r_1, r_2)$ between crystals of size r_1 and r_2, integrated over the crystal size distribution. Thus

$$\dot{E}_t = \int_0^\infty \int_0^\infty q(r_1, r_2)\, E(r_1, r_2)\, n(r_1)\, n(r_2)\, dr_1\, dr_2 \,. \tag{101}$$

For simplicity, the crystal size distribution function, n, will be written as a function of the crystal size only. We determine the collision frequency per unit volume between crystals of size r_1 to $r_1 + dr_1$ and size r_2 to $r_2 + dr_2$ as follows. Let $R_c = (r_1 + r_2)$ be the "collision radius," and $\Psi(r_1, r_2)$ be the

collision efficiency of crystals of size r_1 and r_2. The collision efficiency is defined as the portion of crystals that would have collided if the fluid flow field hadn't been distorted by the crystals (Saffman and Turner 1956). Assume that the coordinate system is centered on one particle and is moving with the steady velocity of the particle. Let $v(r_1, r_2)$ be the relative motion between the crystals in this coordinate system. Thus

$$q(r_1, r_2) = \pi(r_1+r_2)^2 \, v(r_1, r_2) \, \Psi(r_1, r_2) \tag{102}$$

and by this definition, $v(r_1, r_1) \geq 0$.

We can estimate the collision energy by determining the energy exchanged between crystals of sizes r_1 and r_2 during a collision. Again, take one crystal to be the origin of the coordinate system, say r_2. The relative velocity between r_1 and r_2 will be $v(r_1, r_2)$. When the crystals collide they will deform plastically and elastically; their centers will come together and approach a minimum distance. We will assume that the collision is inelastic enough so that when the distance between the centers of the crystals is a minimum, the crystals will not be moving relative to one another. They will then be moving together at some resultant velocity $\bar{v}$. A momentum balance is

$$m(r_1) \, v(r_1, r_2) = [m(r_1) + m(r_2)] \, \bar{v} \tag{103}$$

where $m(r_1)$ and $m(r_2)$ are the masses of the two crystals with size r_1 and r_2 respectively. The magnitude of the energy expended in the collision will be equal to the difference in the kinetic energy of the two crystals before and after the collision, or

$$E(r_1, r_2) = \tfrac{1}{2} \, m(r_1) \, v^2(r_1, r_2) - \tfrac{1}{2} \, [m(r_1) + m(r_2)] \, \bar{v}^2. \tag{104}$$

Substituting from eq 103, we find

$$E(r_1, r_2) = \tfrac{1}{2} \, \frac{m(r_1) \, m(r_2)}{m(r_1) + m(r_2)} \, v^2(r_1, r_2). \tag{105}$$

The rate of energy transfer can now be expressed as

$$\dot{E}_t = \int_0^{\infty} \int_0^{\infty} \frac{\pi}{2} \, (r_1+r_2)^2 \, \frac{m(r_1) \, m(r_2)}{[m(r_1) + m(r_2)]} \, \Psi(r_1, r_2) \, v^3(r_1, r_2) \, n(r_1) \, n(r_2) \, dr_1 \, dr_2 \tag{106}$$

and it now remains for us to determine the relative velocity and collision efficiency applicable to each mechanism of collision.

Collisions from the crystals moving with the fluid. For this analysis we will assume that the crystals exactly follow the fluid motion, that is, all inertial buoyancy and other effects are ignored. As in the *Ice Crystal Growth Rates* section, it will be necessary to analyze the dissipative and inertial subranges separately.

If $R_c < \eta$, then we can estimate the rate of energy transfer assuming that both crystals are in the dissipative subrange. The mean square relative velocity between two points separated by a distance R_c, where $R_c < \eta$, is

$$v(r_1, r_2) = 0.13 \, R_c (\epsilon/\nu)^{1/2}. \tag{107}$$

If $R_c > \eta$, then the relative velocity cannot be estimated as neatly as above. It may be that r_1 or r_2 or both are greater than η. We will assume that if $R_c > \eta$, then the crystals will move with a relative velocity appropriate to the inertial subrange, regardless of each individual crystal's size. The mean square velocity difference between points separated by a distance R_c where $R_c > \eta$ is

$$v(r_1, r_2) = 2.7(\epsilon R_c)^{1/3}. \tag{108}$$

The collision efficiency $\Psi(r_1, r_2)$ is difficult to estimate. Levich (1962) discusses the problem of determining the collision efficiency of suspended particles. Complications arise because neither particle is stationary, because turbulence and the boundary layers around the particles modify the fluid stream lines, because inertial forces on the particles must be accounted for, etc. Pruppacher and Klett (1978) discuss the uncertainties of calculating the collision efficiencies of water drops in air. From experimental evidence, Saffman and Turner (1956) assumed that the collision efficiency was unity for collisions between particles of nearly equal size when $R_c < \eta$. However, the discussions of Pruppacher and Klett (1978) indicate that this may not always be true. In general, the collision efficiency goes to zero as r_1/r_2 goes to zero. As r_1 approaches r_2, the collision efficiency rapidly rises to a maximum which may equal unity, and then may increase or decrease as r_1 becomes exactly equal to r_2. In short, estimation of collision efficiency must be an uncertain undertaking. Therefore, we will arbitrarily set the collision efficiency equal to unity, but not without reservations. When $r_2 \gg r_1$, the energy of the collision will be proportional to

$$\frac{m(r_1)\,m(r_2)}{m(r_1)+m(r_2)} \approx m(r_1) \tag{109}$$

and so will be very small, as $m(r_1) \approx r_1^3$. Therefore, the error introduced by not having $\Psi(r_1, r_2)$ go to zero as r_1/r_2 goes to zero should be small.

Substituting the above expressions into the rate of energy transfer, we see that for $R_c < \eta$

$$\dot{E}_t = (0.003)(\epsilon/\upsilon)^{3/2} \int_0^\infty \int_0^\infty (r_1+r_2)^5 \frac{m(r_1)\,m(r_2)}{[m(r_1)+m(r_2)]}\, n(r_1)\, n(r_2)\, dr_1\, dr_2 \tag{110}$$

and for $R_c > \eta$

$$\dot{E}_t = (30.92)(\epsilon) \int_0^\infty \int_0^\infty (r_1+r_2)^3 \frac{m(r_1)\,m(r_2)}{[m(r_1)+m(r_2)]}\, n(r_1)\, n(r_2)\, dr_1\, dr_2\,. \tag{111}$$

Collisions caused by buoyancy. When the density of the crystals is not identical to that of the fluid, the crystals will move relative to the fluid under the influence of gravity. This motion will be in addition to all other motions of the crystals. In the *Heat Transfer from Ice Crystals Suspended in Turbulent Water* section, the relative velocity induced by gravity was determined. Using the intermediate law for calculating the drag coefficient, we can find the terminal rise velocity of a crystal to be

$$U_t = (0.16 g'^{0.715}/\upsilon^{0.428})\, r^{1.14} \tag{112}$$

and the relative velocity $v(r_1, r_2)$ is therefore

$$v(r_1, r_2) = (0.16 g'^{0.715}/\upsilon^{0.428})(|r_1^{1.14} - r_2^{1.14}|). \tag{113}$$

Again collision efficiency will be equal to unity. Thus

$$\dot{E}_t = (0.16 g'^{0.715}/\upsilon^{0.428})^3(\pi/2) \int_0^\infty \int_0^\infty (r_1+r_2)^2 \frac{m(r_1)\,m(r_2)}{[m(r_1)+m(r_2)]}$$

$$(|r_1^{1.14} - r_2^{1.14}|)^3\, n(r_1)\, n(r_1)\, n(r_2)\, dr_1\, dr_2. \tag{114}$$

Crystal-boundary collisions

The second general class of collisions are those between the crystals and the external boundaries. To determine the frequency of crystal-boundary collisions requires knowledge of the size and shape of the water body of interest. As this report is intended to be as general as possible, this knowledge cannot be assumed; however, this section is presented in the interest of completeness.

The experiments of Evans et al. (1974b) demonstrated that collisions between ice crystals and the walls, baffles and impeller of the crystallizer were a significant cause of secondary nucleation. They assumed that any crystal moving with the bulk flow could potentially collide with the impeller, and any crystal closer than an eddy size away from the wall could collide with the wall. They were unable to determine if either collision mechanism dominated, but they did find that coating the metal surfaces of the impeller and crystallizer with a soft material substantially reduced the nucleation rate.

In natural water bodies, collisions with external boundaries are probably not a significant cause of secondary nucleation except in some circumstances. First of all, the ratio of surface area to volume of most natural water bodies is much smaller than that of a crystallizer. Also, the boundaries of natural water bodies tend to be very rough compared to crystallizers. Crystals colliding with these rough boundaries tend to stick and remain at the boundary, which results in the buildup of anchor ice. Therefore, only in locations such as shallow, rocky rapids could crystal-boundary collisions be important.

The rate of energy transfer during the collision of a crystal with a boundary may be crudely estimated in the following manner. This analysis does not account for the effects of a boundary layer, inertia, etc. Let ℓ_m be the maximum eddy size that can bring crystals into contact with the boundary. Assume that the number density of crystals is uniform throughout the region. The probability that a crystal of size r exists in the region within a distance close enough to collide with a boundary is

$$\text{prob.} \approx \frac{\ell_m}{R_h} \int_0^r n(r)\, dr \tag{115}$$

where R_h is the hydraulic radius, or the ratio of volume to surface area. The relative velocity of the crystal and the boundary can be estimated as

$$U_{rb} \approx (\epsilon\, \ell_m)^{1/3} \tag{116}$$

and the energy at collision

$$E_{rb} = \tfrac{1}{2}\, m(r)\, v_{rb}^2 = \tfrac{1}{2}\, m(r)\, (\epsilon\, \ell_m)^{2/3}. \tag{117}$$

Now the rate of collisions will be proportional to

$$q_{rb} \approx \frac{(\epsilon\, \ell_m)^{1/3}}{\ell_m} \frac{\ell_m}{R_h} \int_0^r n(r)\, dr \tag{118}$$

and thus

$$\dot{E}_t \approx \frac{\epsilon}{2} \frac{\ell_m}{R_h} \int_0^r m(r)\, n(r)\, dr. \tag{119}$$

Summary

In this section the kinetics of secondary nucleation has been partially modeled. Starting from a theoretical formulation of the rate of secondary nucleation, we find

$$\dot{N}_t = (\dot{E}_{t1}+\dot{E}_{t2}+\dot{E}_{t3}+\ldots)\, S_N(\theta, \epsilon, C_T, \text{etc.}).$$

The rate of energy transfer $\dot{E}_{ti}$ has been determined for several different mechanisms of collision. The function S_N is necessarily empirical at this time because we know of no way to calculate its value theoretically. S_N is the product of two functions: F_1, the number of particles produced per unit of collision energy and F_2, the number of particles surviving to become crystals. We expect that F_1 should be a linear function of the collision energy and have relatively little dependence on the supercooling or turbulence levels. F_2 should largely depend on the supercooling, in accordance with the survival theory (Garabedian and Strickland-Constable 1974). S_N should largely depend on the supercooling and perhaps depend less on the level of turbulence, ϵ. The experimental results of Evans et al. (1974a, b) are difficult to analyze conclusively. However, they reported that the dependence of S_N on ϵ is small.

The terms in eq 110, 111 and 114 for $\dot{E}_t$ are difficult to compare with each other. To facilitate a comparison, let $\bar{r}$ be the average crystal size, specified in any convenient manner. Then let r^* be the nondimensional crystal size, defined as

$$r^* = r/\bar{r}\,. \tag{120}$$

We will assume that the crystal size distribution can be expressed as

$$n(r) = N(0)\, T(r/\bar{r}) \tag{121}$$

where $T(r/\bar{r})$ defines the form of the crystal size distribution and is constant with time; $N(0)$ is the number of crystals of a size $r = 0$. When the form of the size distribution is fixed, specifying the number of crystals of any size determines the number of all other sizes. Expressing the size distribution in this way is a simplification introduced purely as a device to facilitate comparison of the mechanisms of collision. It may not be possible to do this in actual practice, as the form of the size distribution may vary with time.

For example, introducing eq 120 and 121 into 110 and noting $m(r) = \rho_i K_v r^3$, we see that

$$\dot{E}_t = (0.003)(\epsilon/\upsilon)^{3/2}\rho_i K_v \bar{r}^{8.0} N(0)^2 \int_0^\infty\int_0^\infty (r_1^* + r_2^*)^5 \frac{r_1^{*3}+r_2^{*3}}{(r_1^{*3}+r_2^{*3})}\, T(r_1^*)\, T(r_2^*) dr_1\, dr_2\,. \tag{122}$$

Inside the integral are only nondimensional terms and the value of the integral will be a constant with time. Combining all constants, we can now write eq 122

$$\dot{E}_t = a_1(\epsilon/\upsilon)^{3/2}\,\bar{r}^{8.0} \tag{123}$$

and in the same manner we can write eq 111 and 114 for $R_c > \eta$

$$\dot{E}_t = a_2\,\epsilon\bar{r}^{6.0} + a_3\bar{r}^{8.42}. \tag{124}$$

The first term on the right side of each expression is the rate of energy transfer due to crystal-crystal collisions. The second term in eq 124 is that due to crystal-crystal collisions caused by gravity. The rate due to crystal-boundary collisions has not been included here, as its determination requires knowledge of the particular water body. The magnitudes of $\dot{E}_t$ are nonlinear functions of the form and magnitude of the crystal size distributions. It is easy to see that small changes in the crystal size distribution could cause very large changes in the rate of secondary nucleation. The sudden appearance of vast numbers of frazil crystals, observed both in natural water bodies and experimentally, may be a result of this large nonlinearity in the rate of secondary nucleation.

FRAZIL ICE DYNAMICS

Introduction

In this report the mathematics of the formation of frazil ice, the basic equations and expressions for the important parameters, were developed. Much work remains to be done. The author hopes that the synthesis contained in this report will provide insights into the phenomenon of frazil and provide a foundation for further work.

This section presents a simple but practical example of the crystal number continuity equation and the heat balance.

Steady-state crystal number continuity equation and heat balance in a MSMPR crystallizer

Equation 9 can be specifically and practically applied to a mixed suspension, mixed product removal (MSMPR) crystallizer operating at steady state. This application results in the most widely known and used analytical solution to eq 9. Because of the generality of eq 9, it is not in the best form for this particular application. A very usable form can be achieved by integrating this equation over the macroscopic volume $V(t)$ in the external coordinate subregion that corresponds to the volume of the MSMPR crystallizer. To carry out this integration, the volume of the crystallizer must be well mixed. That is, in any arbitrary small element of its volume, a full and representative crystal population distribution that is dependent only on the internal coordinate must exist. Within this volume, the population density function $n(R, t)$ can be written $n(r, t)$ as it has no dependence on the spatial coordinates. $n(r)$ can now be interpreted as a size distribution function. In addition, G, B and D are also required to be independent of the spatial coordinates within this volume. Therefore multiplying eq 9 by dV and integrating over $V(t)$, we obtain

$$\int_V \left[\frac{\partial n}{\partial t} + \nabla(\vec{V}_e n) + \frac{\partial}{\partial r}(Gn) + D - B\right] dV = 0. \tag{125}$$

Every term can be removed from the integral except for the second, which results in an integral over the volume of the spatial divergence of the population flux. This term can be converted into a surface integral of the population flux flowing through the surface of the volume $V(t)$, which in principle may not be stationary. This results in

$$\int_V \nabla(\vec{V}_e n) dV = \sum_K Q_K n_K + \frac{n dV}{dt} \tag{126}$$

where Q_K is the flow rate and n_K the population density of the K^{th} input and output stream into $V(t)$. Carrying out the integration of eq 125 and dividing by $V(t)$, we find

$$\frac{\partial n}{\partial t} + \frac{\partial}{\partial r}(Gn) + D - B + n\frac{d \log V(t)}{dt} = -\sum_K \frac{Q_K n_K}{V(t)} \quad . \tag{127}$$

This is the number continuity equation integrated over a macroscopic external volume. It is averaged in the external phase space and distributed in the internal phase space.

In the same manner the heat balance equation (eq 16b) can be integrated over the macroscopic volume of the crystallizer. This results in

$$\frac{\partial \theta}{\partial t} = \frac{L}{C\rho_f}\frac{\partial \hat{\rho}_i}{\partial t} - \sum_K \frac{Q_K \theta_K}{V} + L\sum_K \frac{Q_K \hat{\rho}_{iK}}{VC\rho_f} + \frac{\bar{Q}^*}{C\rho_f} \tag{128}$$

where $\hat{\rho}_{iK}$ is the mass density of ice in the K^{th} input or output stream into $V(t)$.

The following assumptions regarding the operation of the MSMPR crystallizer can now be made.

1. The volume of the crystallizer does not change with time. This requires that the volume of crystals be small compared to the total volume (a thin suspension).
2. The remaining time-dependent terms can be dropped as the crystallizer operates at steady state.
3. The birth and death functions can be set to zero for all sizes of crystals.
4. The crystallizer can be assumed to operate with clear or unseeded feed streams. Also, the size distribution of crystals in the outflow is exactly identical to the distribution in the crystallizer. The ratio $V(t)/\sum_K Q_K$ can then be interpreted as the flow-through time, τ.
5. McCabe's law is assumed to hold. This law, often applied under the conditions found in industrial crystallizers, requires that the growth rate not be a function of the crystal size.
6. The population density of newly nucleated crystals will be defined as n^0 and will be assumed constant. We assume the size of the nucleated crystals to be vanishingly close to zero. n^0 is the lower boundary condition for the crystal size distribution. The relationship between n^0 and the secondary nucleation rate $\dot{N}_I$ is

$$n^0 = (\dot{N}_I/G). \tag{129}$$

Equations 127 and 128 can now be written

$$G\frac{\partial n}{\partial r} + \frac{n}{\tau} = 0 \tag{130}$$

$$C\rho_f\left(\frac{\theta_{in} - \theta_{out}}{\tau}\right) = \frac{L\dot{\rho}_i}{\tau} + \bar{Q}^*. \tag{131}$$

Separating variables and integrating eq 129, we obtain

$$\int_{n^0}^{n} (dn/n) = -\int_0^r (dr/G\tau) \tag{132}$$

which gives

$$n(r) = n^0 \exp(-r/G\tau) \tag{133}$$

and, from eq 131, assuming $\theta_{in} = \theta_{out}$ gives us

$$\dot{\rho}_i = -(\bar{Q}^*/L)\tau. \tag{134}$$

Crystal size distributions of MSMPR crystallizers operating at steady state are often very close to the size distributions of eq 133. This provides a convenient graphic method of determining the growth rates and the density of nucleated crystals by plotting the log of measured population density against the crystal size r. The graph is a straight line with intercept of $\log n^0$ and slope of $-(G\tau)^{-1}$. Additional information can be obtained about the growth rates, the mass of crystals or other aspects of the crystallizer operation. For example, noting that

$$\dot{\rho}_i = \rho_i K_v \int_0^\infty r^3\, n(r)\, dr$$

substituting the distribution for $n(r)$ from eq 133 and solving for G, we get

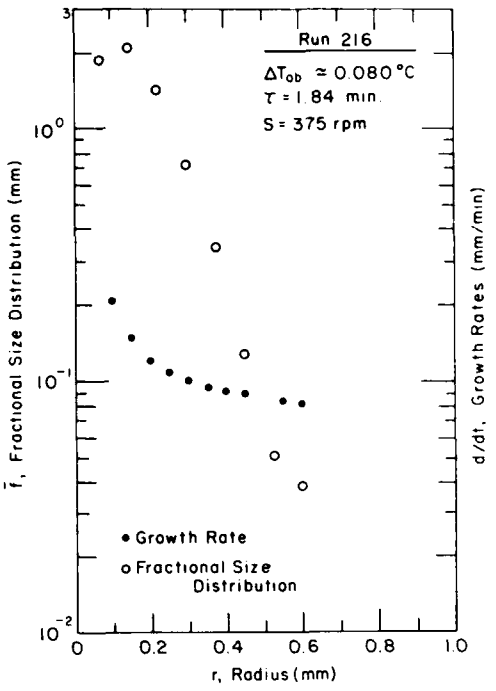

Figure 9. Frazil crystal size distribution and growth rate (after Smith and Sarofim 1979).

$$G = \left(\frac{\bar{Q}^*}{6n^0 K_v L \rho_i \tau^3}\right)^{1/4} \quad (135)$$

Increasing the rate at which heat is removed or decreasing the residence time will increase the average growth rate of the crystals. It is in this manner that the operations of such crystallizers are studied to determine their operating characteristics.

As was seen in the *Ice Crystal Growth Rates* section, the growth rate is not constant with crystal size. This will cause the crystal size distribution to deviate from the straight line of eq 133. If the growth rate varies with crystal size, eq 129 is written

$$\frac{\partial(Gn)}{\partial t} + \frac{n}{\tau} = 0.$$

This equation can be solved as the difference in the product of the growth rate and the distribution at any two sizes

$$(Gn)r_1 - (Gn)r_2 = -(1/\tau)\int_{r_2}^{r_1} n(r)dr.$$

This expression allows the variable growth rate to be determined from the measured crystal size distribution if the growth rate at any size is known. An example of such data is shown in Figure 9.

SUMMARY AND FUTURE WORK

Overview

The equations describing the dynamic interaction of the crystal distribution and the heat balance of the water were developed in the *Basic Equations* section. Randolph and Larson (1971) used the term "information" to describe the crystal distribution and the heat balance. "Frazil ice dynamics" describes the unique internal information feedback loop that regulates the crystal size distribution. The mechanism for this information feedback is through the level of supercooling resulting from the balance of the latent heat released by the production of ice and the total heat loss from the water. The supercooling level of the water ultimately determines the rates of secondary nucleation and crystal growth, which in turn determine the dynamic crystal distribution at any time. The level of turbulence controls the rate at which the feedback loop can operate. This is shown graphically in Figure 10.

The two basic environmental parameters are the rate of heat loss from the water and the level of turbulence of the water. The rate of heat loss can be thought of as a disturbance that manifests in the supercooling of the water. The crystal distribution develops in response to this disturbance and its ultimate effect is to eliminate the disturbance and return the temperature of the water to the freezing point. The level of turbulence controls the rate at which the crystal distribution can respond to the disturbance. The level of supercooling is determined by both the rate of cooling and the level of turbulence. Increasing the level of turbulence will tend to decrease the level of supercooling. This may have profound implications for engineers who design water intakes that must

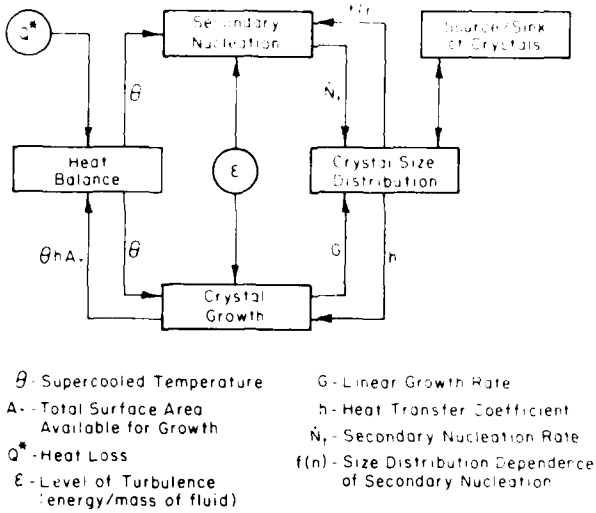

Figure 10. Frazil ice dynamics.

operate in winter. This interaction between the rate of heat loss, turbulence and supercooling was suggested in the experiments of Carstens (1966).

Basic equations

The basic equations describing the crystal number continuity equation and the heat balance of the water were developed in the *Basic Equations* section. Simple versions of the heat balance have been applied to the formation of frazil ice in natural water bodies by previous researchers (Osterkamp 1978). The number continuity equation has not been applied, and it is unclear at this point what the resulting distribution will be. The size distribution of frazil crystals has not been measured for any water body under any conditions. These are the first vital field data that should be collected. The hydraulic and meteorologic conditions under which the size distribution is measured should be carefully determined. Parallel to this effort, the solution of the basic equations should be pursued. Currently, the solution of these equations cannot be considered routine. The numerical schemes necessary for their solution must be developed and tested.

The importance to the crystal distribution of such physical processes as the formation of anchor ice and flocculation of the frazil disks is not yet known. These processes must be investigated and their influences assessed.

Growth rates

Despite much effort, the intrinsic kinetics of ice crystal growth has not been completely determined. This is the one major potential problem in determining the growth rate of ice. Determination of the crystalline kinetics requires carefully controlled experiments in which a water temperature can be accurately maintained and measured. For growth controlled by heat transfer, the growth rates can be estimated fairly well. However, the transfer rates in the inertial subrange have been determined based on the Frössling equation, an experimentally based relationship. The development of a rational theory of transfer rates in this region is needed.

Nucleation rates

The nucleation rates of frazil ice crystals are probably the largest unknown at this time. The existence of secondary nucleation of frazil ice in natural water bodies has been conjectured (Osterkamp 1977) but not yet demonstrated. The development of a theoretical basis for the determination of the number of nuclei produced per unit collision energy is needed as is a rigorous testing of the survival theory and experimental confirmation of the collision rates.

LITERATURE CITED

Acrivos, A. and T.D. Taylor (1962) Heat and mass transfer from single spheres in Stokes flow. *Physics of Fluids*, **5**(4): 387–394.

Altberg, W.J. (1936) Twenty years of work in the domain of underwater ice formation (1915–1935). International Union of Geodesy and Geophysics, International Association of Scientific Hydrology, Bulletin No. 23, pp. 373–407.

Arakawa, K. (1954) Studies on the freezing of water. II. Formation of disc crystals. *Journal of the Faculty of Science, Hokkaido University*, Series II, **IV**(5): 310–339.

Arden, R.S. and T.E. Wigle (1972) Dynamics of ice formation in the Upper Niagara River. In *International Symposium on the Role of Snow and Ice in Hydrology, Banff, Alberta*. UNESCO-WMO-IHAS, vol. 2.

ASCE Task Committee on Hydromechanics of Ice of the Committee on Hydromechanics (1974) River ice problems: A state-of-the-art survey and assessment of research needs. *Journal of the Hydraulics Division, ASCE*, 100(HY1): 1–15.

Ashton, G.D. (1978) River ice. *Annual Review of Fluid Mechanics*, **10**: 369–392.

Barnes, H.T. (1928) *Ice Engineering*. Montreal: Renouf Publishing Company.

Batchelor, G.K. (1953) *The Theory of Homogeneous Turbulence*. London: Cambridge University Press.

Batchelor, G.K. (1979) Mass transfer from a particle suspended in fluid with a steady linear ambient velocity distribution. *Journal of Fluid Mechnics*, **95**(2): 369–400.

Batchelor, G.K. (1980) Mass transfer from small particles suspended in turbulent fluid. *Journal of Fluid Mechanics*, **98**(3): 609–623.

Botsaris, G.D. (1976) Secondary nucleation – A review. In *Industrial Crystallization* (J.W. Mullin, Ed.). New York: Plenum Press.

Brenner, H. (1963) Forced convection heat and mass transfer at small Péclet numbers from a particle of arbitrary shape. *Chemical Engineering Science*, **18**: 109–122.

Brian, P.L.T. and H.B. Hales (1969) Effects of transpiration and changing diameter on heat and mass transfer to spheres. *American Institute of Chemical Engineers Journal*, **15**(3): 419–425.

Carslaw, H.S. and J.C. Jaeger (1959) *Conduction of Heat in Solids*, 2nd edition. London: Oxford University Press.

Carstens, T. (1966) Experiments with supercooling and ice formation in flowing water. *Geofysiske Publikasjoner*, **26**(9): 3–18.

Carstens, T. (1970) Heat exchanges and frazil formation. In *Proceedings of the Symposium on Ice and Its Action on Hydraulic Structures, Reykjavik, Iceland*. International Association for Hydraulic Research, Paper no. 2.11.

Clontz, N.A. and W.L. McCabe (1972) Contact nucleation of magnesium sulfate heptahydrate. *Chemical Engineering Progress, Symposium Series*, No. 110, **67**(6).

Denk, E.G. and G.D. Botsaris (1972) Mechanism of contact nucleation. *Journal of Crystal Growth*, **15**: 57–60.

Desai, R.M., J.W. Rachow and D.C. Timm (1974) Collision breeding: A function of crystal moments and degree of mixing. *American Institute of Chemical Engineers Journal*, **20**(1): 43–50.

Dorsey, N.E. (1948) The freezing of supercooled water. *Transactions of the American Philosophical Society*, **38**(3): 245–328.

Evans, T.W. (1973) Mechanisms of secondary nucleation during the crystallization of ice. Ph.D. Dissertation, Department of Chemical Engineering. Cambridge: Massachusetts Institute of Technology.

Evans, T.W., G. Margolis and A.F. Sarofim (1974a) Mechanisms of secondary nucleation in agitated crystallizers. *American Institute of Chemical Engineers Journal*, **20**(5): 950–958.

Evans, T.W., A.F. Sarofim and G. Margolis (1974b) Models of secondary nucleation attributable to crystal-crystallizer and crystal-crystal collisions. *American Institute of Chemical Engineers Journal*, **20**(5): 959–966.

Ferguson, H.L. and H.F. Cork (1972) Regression equations relating ice conditions in the Upper Niagara River to meteorological variables. In *International Symposium on the Role of Snow and Ice in Hydrology, Banff, Alberta.* UNESCO-WMO-IAHS, vol. 2.

Fletcher, N.H. (1970) *Chemical Physics of Ice.* London: Cambridge University Press.

Freysteinsson, S. (1970) Calculation of frazil ice production. In *Proceedings of the Symposium on Ice and Its Action on Hydraulic Structures, Reykjavik, Iceland.* International Association for Hydraulic Research, Paper no. 2.1.

Fujioka, T. and R.F. Sekerka (1974) Morphological stability of disc crystals. *Journal of Crystal Growth,* **24/25**: 84-93.

Garabedian, H. and R.F. Strickland-Constable (1972) Collision breeding of crystal nuclei: sodium chlorate. *Journal of Crystal Growth,* **12**: 53-56.

Garabedian, H. and R.F. Strickland-Constable (1974) Collision breeding of ice crystals. *Journal of Crystal Growth,* **22**: 188-192.

Garside, J. and M.A. Larson (1978) Direct observation of secondary nuclei production. *Journal of Crystal Growth,* **43**: 694-704.

Gilfillian, R.E., W.L. Kline, T.E. Osterkamp and C.S. Benson (1972) Ice formation in a small Alaskan stream. In *International Symposium on the Role of Snow and Ice in Hydrology, Banff, Alberta.* UNESCO-WMO-IAHS, vol. 2.

Gilpin, R.R. (1976) The influence of natural convection on dendritic ice growth. *Journal of Crystal Growth,* **36**: 101-108.

Granbois, K.J. (1953) Combating frazil ice in hydro-electric stations. *Power Apparatus and Systems,* **5**: 111-116.

Hillig, W.B. (1958) The kinetics of freezing of ice in the direction perpendicular to the basal plane. In *Growth and Perfection of Crystals* (R.H. Dormus, B.W. Roberts and D. Turnbull, Eds.). New York: J. Wiley and Sons.

Hinze, J.O. (1959) *Turbulence.* New York: McGraw-Hill.

Hobbs, P.V. (1974) *Ice Physics.* London: Oxford University Press.

Jackson, K.A., D.R. Uhlmann and J.D. Hunt (1967) On the nature of crystal growth from the melt. *Journal of Crystal Growth,* **1**: 1-36.

Kallungal, J.P. and A.J. Barduhn (1977) Growth rate of an ice crystal in subcooled pure water. *American Institute of Chemical Engineers Journal,* **23**(3): 294-303.

Kane, S.G. (1971) Secondary nucleation of ice in a stirred batch crystallizer. Ph.D. Dissertation. Department of Chemical Engineering. Cambridge: Massachusetts Institute of Technology.

Kuboi, R., I. Komasawa and T. Otake (1974) Fluid and particle motion in turbulent dispersion. II. Influence of turbulence of liquid on the motion of suspended particles. *Chemical Engineering Science,* **29**: 651-657.

Kumai, M. and K. Itagaki (1953) Cinematographic study of ice crystal formation in water. *Journal of the Faculty of Science, Hokkaido University,* Series II, **IV**(4): 234-246.

Lal, D.P., R.E.A. Mason and R.F. Strickland-Constable (1969) Collision breeding of crystal nuclei. *Journal of Crystal Growth,* **5**: 1-8.

Lavender, W.J. and D.C.T. Pei (1967) The effect of fluid turbulence on the rate of heat transfer from spheres. *International Journal of Heat and Mass Transfer,* **10**: 529-539.

Levich, V.G. (1962) *Physiochemical Hydrodynamics.* Englewood Cliffs, N.J.: Prentice-Hall.

List, R. and L.A. Barrie (1972) Heat losses and synoptic patterns relating to frazil ice production in the Niagara River. In *International Symposium on the Role of Snow and Ice in Hydrology, Banff, Alberta.* UNESCO-WMO-IAHS, vol. 2.

Logan, T.H. (1974) Prevention of frazil ice clogging of water intakes by application of heat. U.S. Department of Interior, Bureau of Reclamation, REC-ERC-74-15.

Margolis, G. (1969) The nucleation and growth rates of ice in a well-stirred crystallizer. Ph.D. Dissertation. Department of Chemical Engineering. Cambridge: Massachusetts Institute of Technology.

Martin, S. (1981) Frazil ice in rivers and oceans. *Annual Review of Fluid Mechanics,* **13**: 379-397.

Michel, B. (1963) Theory of formation and deposit of frazil ice. *Eastern Snow Conference, Proceedings of the 1963 Annual Meeting, Quebec City.*

Michel, B. (1971) Winter regime of rivers and lakes. USA Cold Regions Research and Engineering Laboratory, Cold Regions Science and Engineering Monograph III-B1a. AD 724121.

Muller, A. (1978) Frazil ice formation in turbulent flow. Iowa Institute of Hydraulic Research, Report No. 214.

Murphy, J. (1909) The ice question as it effects Canadian water powers with special reference to frazil and anchor ice. *Transactions of the Royal Society of Canada,* Section III, 143-177.

Osterkamp, T.E. (1977) Frazil-ice nucleation by mass-exchange processes at the air/water interface. *Journal of Glaciology,* **19**(81): 619-625.

Osterkamp, T.E. (1978) Frazil ice formation: A review. *Journal of the Hydraulics Division, ASCE,* 104(HY9): 1239-1255.

Osterkamp, T.E. and R.E. Gilfillian (1975) Nucleation characteristics of stream water and frazil ice nucleation. *Water Resources Research,* **11**(6): 926-928.

Ottens, E.P.K., A.H. Janse and E.S. DeJong (1972) Secondary nucleation in a stirred vessel cooling crystallizer. *Journal of Crystal Growth,* **13/14**: 500-505.

Paulson, C.A. and J.J. Simpson (1981) The temperature difference across the cool skin of the ocean. *Journal of Geophysical Research,* **86**(C11): 11,044-11,054.

Piotrovich, V.V. (1956) Formation of depth ice. *Priroda,* **9**: 94-95. (Translated by Defense Research Board, DSIS, Department of National Defense, Canada.)

Pruppacher, H.R. and J.D. Klett (1978) *Microphysics of Clouds and Precipitation.* Boston: D. Reidel Publishing Company.

Randolph, A.D. and M.A. Larson (1971) *Theory of Particulate Processes.* New York: Academic Press.

Saffman, P.G. and J.S. Turner (1956) On the collision of drops in turbulent clouds. *Journal of Fluid Mechanics,* **1**: 16-30.

Schaefer, V.J. (1950) The formation of frazil and anchor ice in cold water. *Transactions of the American Geophysical Union,* **31**(6): 885-893.

Shen, H.T. (1980) Surface heat loss and frazil ice production in the St. Lawrence River. *Water Resources Bulletin,* **16**(6): 996-1001.

Shen, H.T. and R.W. Ruggles (1982) Winter heat budget and frazil ice production in the Upper St. Lawrence River. *Water Resources Bulletin,* **18**(2): 251-257.

Simpson, H.D., G.C. Beggs, J. Deans and J. Nakamura (1973) The growth of ice crystals. *4th International Symposium on Fresh Water from the Sea,* **3**: 395-407.

Smith, K.A. and A.F. Sarofim (1979) Fundamental studies of desalination by freezing. Final Report to Office of Water Research and Technology, U.S. Department of Interior, Washington, D.C.

Sperry, P.R. (1965) The effects of additives on the kinetics of crystallization of supercooled water. Ph.D. Dissertation. Department of Chemical Engineering. Cambridge: Massachusetts Institute of Technology.

Tantillo, T. (1981) Hydraulic model study of a water intake under frazil ice conditions. USA Cold Regions Research and Engineering Laboratory, CRREL Report 81-3. ADA 099171.

Tennekes, H. and J.L. Lumley (1972) *A First Course in Turbulence.* Cambridge, Mass: MIT Press.

Wadia, P.H. (1974) Mass transfer from spheres and discs in turbulent agitated vessels. Ph.D. Dissertation. Department of Chemical Engineering. Cambridge: Massachusetts Institute of Technology.

Wigle, T.E. and R.S. Arden (1970) Investigations into frazil, bottom ice and surface ice formation in the Niagara River. In *Proceedings of the Symposium on Ice and Its Action on Hydraulic Structures, Reykjavik, Iceland.* International Association for Hydraulic Research, Paper no. 2.8.

Williams, G.P. (1959) Frazil ice: A review of its properties, with a selected bibliography. *The Engineering Journal,* **42**(11): 55-60.

Williamson, R.B. and B. Chalmers (1966) Morphology of ice solidified in undercooled water. In *Crystal Growth* (H.S. Peiser, Ed.). New York: Pergamon Press.

Woltz, F.E. (1975) Crystal surface morphology and secondary nucleation. Ph.D. Dissertation. Department of Chemical Engineering. Cambridge: Massachusetts Institute of Technology.

A facsimile catalog card in Library of Congress MARC format is reproduced below.

Daly, Steven F.
Frazil ice dynamics / by Steven F. Daly. Hanover, N.H.: Cold Regions Research and Engineering Laboratory. Springfield, Va.: available from National Technical Information Service, 1984.
vi, 56 p., illus.; 28 cm. (Monograph 84-1.)
Prepared for the Office of the Chief of Engineers by U.S. Army Cold Regions Research and Engineering Laboratory.
Bibliography: p. 44.
1. Crystal growth. 2. Crystallization. 3. Frazil ice. 4. Ice. 5. Ice formation. 6. Ice prevention. 7. Mathematical analysis. I. United States. Army. Corps of Engineers. II. Cold Regions Research and Engineering Laboratory, Hanover, N.H. III. Series: Monograph 84-1.

8